AD-A047 115 SANDERS ASSOCIATES INC NASHUA N H F/G 13/10
COMPRESSIVE STRENGTH OF SHIP HULL GIRDERS. PART III. THEORY AND--ETC(U)
1977 H BECKER, A COLAO N00024-72-C-5565
UNCLASSIFIED SSC-267 NL

1 OF 1
ADA047115

END
DATE FILMED
1-78
DDC

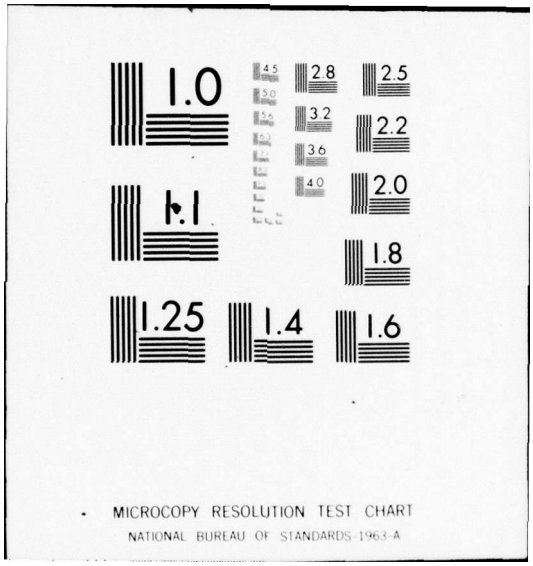
1.0
1.1
1.25
1.4
1.6
1.8
2.0
2.2
2.5
2.8
3.2
3.6
4.0
4.5
5.0
MICROCOPY RESOLUTION TEST CHART
NATIONAL BUREAU OF STANDARDS-1963-A

SSC-267

(1)

B.S.

AD A047115

COMPRESSIVE STRENGTH OF SHIP HULL GIRDERS

PART III

THEORY AND ADDITIONAL EXPERIMENTS

SHIP STRUCTURE COMMITTEE
1977

SHIP STRUCTURE COMMITTEE

AN INTERAGENCY ADVISORY
COMMITTEE DEDICATED TO IMPROVING
THE STRUCTURE OF SHIPS

MEMBER AGENCIES:

UNITED STATES COAST GUARD
NAVAL SHIP SYSTEMS COMMAND
MILITARY SEALIFT COMMAND
MARITIME ADMINISTRATION
AMERICAN BUREAU OF SHIPPING

ADDRESS CORRESPONDENCE TO:

SECRETARY
SHIP STRUCTURE COMMITTEE
U.S. COAST GUARD HEADQUARTERS
WASHINGTON, D.C. 20591

6 September 1977
SR-206

The Ship Structure Committee has been sponsoring an investigation into the ultimate strength of a ship's hull girder under various combinations of longitudinal, transverse, and normal loads in an effort to develop an analytical expression for use by the ship designers.

This report is the third in a series covering the theory and additional experiments on the compressive strength of ship hull girders.

If you have any comments on this report or suggestions for other projects in the ship structure area, they will be most welcome.

W. M. Benkert
Rear Admiral, U. S. Coast Guard
Chairman, Ship Structure Committee

(18) SSC-267 (19)

(9) FINAL TECHNICAL REPORT

on

Project SR-206

"Small Hull Girder Model"

(6) COMPRESSIVE STRENGTH OF SHIP HULL GIRDERS

PART III

THEORY AND ADDITIONAL EXPERIMENTS

by

(10) H. Becker and A. Colao

SANDERS ASSOCIATES, INC.
NASHUA, N.H.

(11) 1977

(12) 79p.

under

Department of the Navy
Naval Ship Systems Command
Contract (15) N00024-72-C-5565

U. S. Coast Guard Headquarters
Washington, D.C.
1977

ABSTRACT

A phenomenological theory has been developed for predicting the ultimate strength of rectangular structural plates loaded in uniaxial longitudinal compression, uniaxial transverse compression and biaxial compression. The effects of normal pressure also were considered.

The theory was found to be in reasonable agreement with experimental data. Certain areas of the theory and some of the experiments require additional study.

The longitudinal compression theory was found to agree well with corresponding theories of other investigators. However, the new theory employs the detailed stress-strain curve for a given material, which the others do not, and demonstrates that, in general, strength prediction requires a curve for each structural material. The commonly used parameter, $(b/t)(\sigma_{cy}/E)^{1/2}$, is shown not to be universally employable across the total material spectrum as the factor identifying ultimate strength.

Other results of broad interest are the demonstration of the applicability of a biaxial plasticity law to biaxial strength theory and the delineation of a method for selecting an optimum material for compression strength.

The use of stress-strain curves for strain analysis of critical and ultimate strengths is described. They were employed to construct theoretical strength curves.

Theoretical relations and corresponding curves have been developed for perfect plates. The effects of strength degrading factors are discussed and the analysis of residual stress effects is included.

CONTENTS

NOMENCLATURE

Symbols

A_y, A_x	Area, in^2
a	Length of plate, in.
b	Width of plate, in. (outside dimensions of tube)
b_e	Effective width of equivalent flange, in.
C	Shell buckling coefficient, figure 22
c	Loss of perfect plate buckling stress
D	Bending stiffness of plate, $Et^3/[12(1-\nu^2)]$, in-lb.
E	Young's modulus, msi (1 msi = 10^6 psi) or psi
E_s, E_t	Secant and tangent moduli, msi or psi
F	$(t/b)(E/\sigma_{cy})^{1/2}$
g	Multiplier converting σ_{cy} to σ_e
h	Number of effective transverse flanges in a plate at biaxial failure
j	Component of plasticity reduction factor
K	$k\pi^2/12[(1-\nu_e^2)]$
k	Buckling coefficient
k_x	Longitudinal buckling coefficient
k_y	Transverse buckling coefficient
ℓ	Multiplier of plate thickness (t) to obtain effective width of weld tension stress region on one side of weld centerline
m	Number of longitudinal half waves in buckled plate
N_x	Plate longitudinal loading, $t\sigma_x = P_x/4b$, lb/in.
N_y	Plate transverse loading, $t\sigma_y = 0.707\ P_y/a$, lb/in.
P_x	Force applied longitudinally to tube, lb. (See sketch, P.69)
P_y	Force applied diagonally transversely to tube, lb. (See sketch, p.69)

p	Pressure acting normal to plate, psi
s	Parameter in theoretical relation for uniaxial longitudinal strength
t	Thickness of plate, in.
w	Deflection normal to prebuckling plane of plate, in.
w_o	Central deflection normal to prebuckling plane of plate, in.
x	Longitudinal coordinate of plate, in.
y	Transverse coordinate of plate, in.
α	Effectiveness factor for transverse postbuckling stresses, eq. (24)
β	(b_e/b)
ε	Strain, microinches/inch (μ)
η	Plasticity reduction factor for inelastic buckling
ν	Poisson's ratio
σ	Stress, ksi

Subscripts

e	Along edge of plate (also elastic when referring to ν)
i	Related to imperfections
p	Related to perfect plate behavior
r	Residual, or related to residual stress
u	Ultimate
v	Related to load variations
x,y,z	Coordinate directions
cr	Critical, or buckling
cy	Compressive yield (in this report a reference to yield is always identified as compressive yield)
pb	Postbuckling

Combined subscripts may be formed from the above. For example:

xcr	x-direction (or longitudinal) critical or buckling
yu	y-direction (or transverse) ultimate

SHIP STRUCTURE COMMITTEE

The SHIP STRUCTURE COMMITTEE is constituted to prosecute a research program to improve the hull structures of ships by an extension of knowledge pertaining to design, materials and methods of fabrication.

RADM W. M. Benkert, USCG (Chairman)
Chief, Office of Merchant Marine Safety
U.S. Coast Guard Headquarters

Mr. P. M. Palermo
Asst. for Structures
Naval Ship Engineering Center
Naval Ship Systems Command

Mr. John L. Foley
Vice President
American Bureau of Shipping

Mr. M. Pitkin
Asst. Administrator for
Commercial Development
Maritime Administration

Mr. C. J. Whitestone
Engineer Officer
Military Sealift Command

SHIP STRUCTURE SUBCOMMITTEE

The SHIP STRUCTURE SUBCOMMITTEE acts for the Ship Structure Committee on technical matters by providing technical coordination for the determination of goals and objectives of the program, and by evaluating and interpreting the results in terms of ship structural design, construction and operation.

NAVAL SEA SYSTEMS COMMAND

Mr. R. Johnson - Member
Mr. J. B. O'Brien - Contract Administrator
Mr. C. Pohler - Member
Mr. G. Sorkin - Member

U.S. COAST GUARD

LCDR E. A. Chazal - Secretary
LCDR S. H. Davis - Member
CAPT C. B. Glass - Member
LCDR J. N. Naegle - Member

MARITIME ADMINISTRATION

Mr. F. Dashnaw - Member
Mr. N. Hammer - Member
Mr. R. K. Kiss - Member
Mr. F. Seibold - Member

MILITARY SEALIFT COMMAND

Mr. T. W. Chapman - Member
CDR J. L. Simmons - Member
Mr. A. B. Stavovy - Member
Mr. D. Stein - Member

AMERICAN BUREAU OF SHIPPING

Mr. S. G. Stiansen - Chairman
Dr. H. Y. Jan - Member
Mr. I. L. Stern - Member

NATIONAL ACADEMY OF SCIENCES
SHIP RESEARCH COMMITTEE

Prof. J. E. Goldberg - Liaison
Mr. R. W. Rumke - Liaison

SOCIETY OF NAVAL ARCHITECTS &
MARINE ENGINEERS

Mr. A. B. Stavovy - Liaison

WELDING RESEARCH COUNCIL

Mr. K. H. Koopman - Liaison

INTERNATIONAL SHIP STRUCTURES
CONGRESS

Prof. J. H. Evans - Liaison

U.S. COAST GUARD ACADEMY

CAPT W. C. Nolan - Liaison

STATE UNIV. OF N.Y. MARITIME COLLEGE

Dr. W. R. Porter - Liaison

AMERICAN IRON & STEEL INSTITUTE

Mr. R. H. Sterne - Liaison

U.S. NAVAL ACADEMY

Dr. R. Bhattacharyya - Liaison

SCOPE OF INVESTIGATION

Purpose of Project

This investigation had the major purpose of developing a usable theory for predicting the strength of rectangular flat plates in polyaxial compression. The theory is developed for materials typical of current and projected ship construction.

An additional purpose of the investigation was to acquire experimental data on materials and plate proportions different from those in the preceding investigation (Ref. 1) in order to provide a broader experimental base from which to test the theory in a critical fashion.

The form of the theory is applicable to a large range of practical ship design problems. It is useful for the construction of design charts and should apply to materials different from those investigated in this project. The general form of the theory contains identification of the material parameters to permit the construction of design charts. However, this investigation has been confined to the development of the basis for the charts. It is considered that chart development is beyond the scope of the current project.

Uniaxial Theory

The primary emphasis throughout the current investigation was on the development of a reasonably clear understanding of the physical character of uniaxial plate strength as determined by laboratory experiments and the manner in which those results relate to the strength of a plate in a ship. For this reason, the technical content of the report begins with an exposition of uniaxial plate strength, to which the primary mass of experimental data pertains.

In this development frequent use is made of the concept of strain analysis of buckling. This requires a detailed understanding of the character of the stress-strain curve and presents related information for several materials including the curves for the materials used in these studies. One of the consequences of the current theory of plate strength is the indication that it is possible to identify the properties of an optimum material for compression strength. This was done using the stress-strain curve alone.

The main stream of the investigation pertains to plates supported on all edges. However, data exist on the strength of flanges which are plates supported on three sides and free on the fourth. The uniaxial theory was extended to that case with good agreement, as will be shown.

The uniaxial theory was compared to experimental data provided by many investigators. The theory not only predicts the behavior of a perfect plate, but also identifies the influence of strength-degrading factors.

When conducting a plate experiment the feature that is most difficult to control is a set of boundary conditions on the plate edges. In a sense, a critical evaluation of a given set of experiments is as much an assessment of the test technique as of the experimental data. For

this reason, an analysis is presented of the procedure used in this investigation and of procedures used by other investigators. The influence of the test method upon the data is discussed. Also important is the comparison of the experiment with the behavior of the plate in a ship grillage.

One of the bounds of plate strength theory is the thick-plate regime in which plastic buckling will occur. A resume of plastic-buckling theory is presented in Appendix III together with some results not previously reported.

Biaxial Theory

When a plate is subjected to both transverse and longitudinal membrane compression the buckling and strength can differ radically from that under uniaxial compression. The biaxial theory addresses this problem with the purpose of identifying a computation technique useful for general analysis and design. The development of the theory depended upon the results of the uniaxial investigations. The results of Ref. 1 are now explicable. The most important result was the identification of a lack of boundary condition control in the previous studies when plates were loaded transversely with no concomitant longitudinal load. Current examinations, in which these boundary conditions were controlled, have shown most of the previous data to agree well with biaxial theory. Furthermore, they have made possible the careful selection of test load combinations to check critically the applicability of the biaxial strength theory during the current test series.

Effect of Normal Pressure

The effect of normal pressure has been separated from membrane strength analysis. If it were possible to develop a basic mathematical procedure (such as plastic finite element analysis), then all these phenomena theoretically could be encompassed in an integrated approach.

In this investigation the effect of normal pressure was identified for the uniaxial case first. Some of the results of Ref. 1 were employed for this purpose. These relate to the shell theory for the strength of compressed plates subjected to normal pressure.

The interaction of normal pressure with plate biaxial strength is apparently considerably more complex. An explanation is offered which is shown to agree reasonably well with observations. However, the requirement for additional research for this area is indicated.

Form of Report

The theoretical approach is based upon features of plate strength, and upon a uniaxial theory, described in previous reports (References 1 and 2). Those reports also contain the seeds of the polyaxial theory developed during the current investigation. It would be possible to present the polyaxial theory by referring to those previous results at pertinent stages in the development of the polyaxial theory. However, it is felt that a more useful purpose would be served by presenting the entire development systematically in this report. The advantage of an integrated approach in one report is felt great enough to outweigh possible objections to some repetition.

The experimental procedure is essentially the same as for Ref. 1. Some modifications have been made to test equipment. These are described in this report. However, the description of the basic procedure has not been repeated. The data from all box experiments appear together with the experimental procedure in Appendix I.

The conclusions and recommendations relate to the degree of understanding of the phenomenology of plate strength under polyaxial loads. Several features require further study. Also, the theory may be tested by comparison with the more fundamental methods of determining plate strength such as the use of finite element analysis. Areas for further study also are delineated.

Discussions are presented on the strengths of grillages, in which rectangular plates of various types provide the load-carrying capacity. In the general survey of Reference 2, the state-of-the-art in grillage strength referred to gaps in the current state of knowledge. Some of those gaps have been partially filled by various investigators as indicated in the discussion in that section which is subsequent to the main stream of the report. No new theoretical approaches are presented. This section primarily contains a discussion of the various modes of grillage strength with emphasis on the use of strain analysis.

Acknowledgment

The authors wish to express appreciation to Mr. W. F. Bierds, Jr., and Mr. R. W. James who designed and built the compression whiffletrees, modified the transverse compression fixtures and pressurization equipment and performed many of the experimental tasks.

UNIAXIAL LONGITUDINAL STRENGTH

Introduction

The uniaxial theory employs a phenomenological model of the post-buckling stress distribution within a plate. The development of the theory was presented in Reference 1. It is repeated here for convenience and also because it forms the basis of the biaxial strength theory.

The procedure to be employed in this section will be the development of the basic theory for supported plates. This will be followed by correlation of theory with existing test data. The same basic approach for simply supported plates has been applied to flanges. The development of the flange theory also will be presented after which a comparison will be shown with flange-strength data.

Hypothetically, maximum strength would be achievable only by a perfect plate, which is defined as a flat plate with no residual stresses under a uniform stress field throughout. Strength-degrading effects are described and are related to observed test results. If degradation is severe enough to obliterate the plate-buckling load-carrying capacity, the plate is classed as poor and the ultimate strength is presumed to be minimal. This applies to plates with large initial imperfections, residual stresses and certain types of loading nonuniformities.

In the process of developing the plate-strength theory use has been made of the critical strain approach to stability analysis. Success with this technique is documented in Reference 1 which shows how the method was used to predict the effects of residual stress.

Plate Failure

The classical description of buckling is the sudden change from the flat state to the bent state. Classical buckling will not occur in a practical plate since it is virtually impossible to avoid imperfections in the plate. As a result, the plate will begin to deflect normal to the plane as soon as load is applied. The buckle height will grow with load. Consequently, the identification of the buckling stress usually involves some mathematical process together with measurement of lateral movement.

Buckling will occur in a flat plate at a load level below that which will induce failure. After the plate buckles in this nonclassical sense, the ability to carry load beyond the critical level is confined mainly to regions near the plate edges if the plate is moderately thick to very thin. When the edge stress level reaches the region of the yield strength of the plate material, the plate is not able to support additional load and collapse occurs. The strength level

is considerably greater than the critical stress level for thin plates, in which buckling will occur elastically. It is essentially the same as the critical stress for thick plates, in which buckling will occur plastically.

The problem of predicting plate strength with an explicit relation is to identify the character of the post-buckling stress at the instant of failure. This was done by von Karman (Reference 3) who confined the load-carrying capacity to the edges, which were assumed to act as flanges operating at the yield strength of the material. Bengtson (Reference 4) amplified that approach by including the buckling stress in the heart of the plate. The theory to be described incorporates the additional stress distribution which would provide a smooth transition from σ_{cy} at the edges to σ_{cr} in the center. Furthermore, it is assumed that the plate may not be perfect and consequently a coefficient is added to reduce the post-buckling stress at the heart of the plate to a value below the critical stress for a perfect plate. This is a consequence of assuming that strength degradation arises from buckling degradation.

Basic Theoretical Approach for Supported Plates

The assumed post-buckling longitudinal membrane stresses in a perfect rectangular plate are shown in Figure 1. The force balance yields

$$b\sigma_{xu} = 2b_e\sigma_{cy} + (b - 2b_e)(1 - c)\sigma_{x\,cr} + 2[\sigma_{cy} - (1 - c)\sigma_{x\,cr}]\int_0^{b/2 - b_e} [y(b/2 - b_e)^{-1}]^s dy \qquad (1)$$

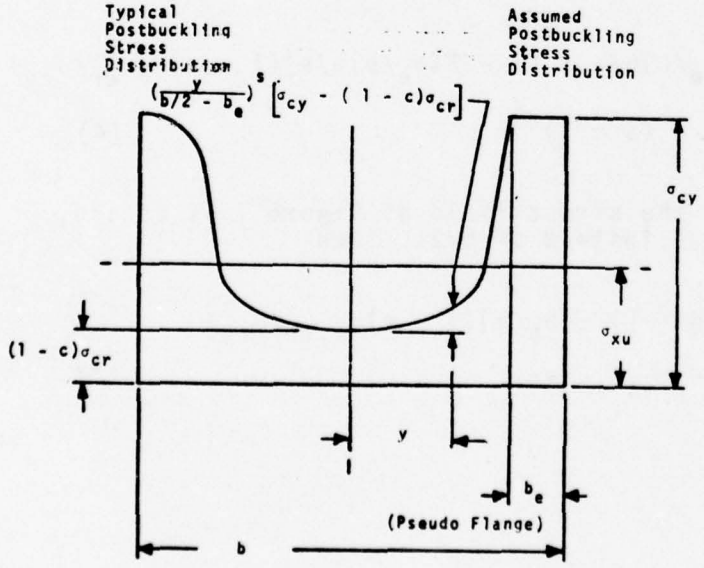

FIGURE 1 LONGITUDINAL POSTBUCKLING STRESS DISTRIBUTION IN SUPPORTED PLATES

The coefficient, c, is the loss of perfect-plate buckling stress which is induced by degrading factors. For a perfect plate c = 0 and for a poor plate c = 1.

When the indicated integration is carried out and Eq. (1) is divided by $b\sigma_{cy}$,

$$\sigma_{xu}/\sigma_{cy} = s(s + 1)^{-1}\{2b_e/b + (1 - 2b_e/b)(1 - c)\sigma_{cr}/\sigma_{cy}\} + (s + 1)^{-1} \tag{2}$$

The general physical character of plate strength may be seen in Eq. (2). For example, when b/t is large (greater than 150, say), then b_e/b and σ_{cr}/σ_{cy} become vanishingly small and

$$\sigma_{xu}/\sigma_{cy} \to (s + 1)^{-1} \tag{3}$$

This makes it possible to select s from the test data at large b/t where the scatter is small. More important, however, is the indication that σ_{xu}/σ_{cy} does not vanish at large b/t.

When $\sigma_{x\ cr}/\sigma_{cy} \to 1$, $\sigma_{xu} \to \sigma_{cy}$. In this regime the theoretical curve from Eq. (2) must agree with values from plastic plate buckling theory.

If a perfect rectangular plate is loaded transversely, Eq. (2) undergoes modification to the form

$$\sigma_{yu}/\sigma_{cy} = s(s + 1)^{-1}\{2(b_e/b)b/a + [1 - 2(b_e/b)b/a](1 - c)\sigma_{y\ cr}/\sigma_{cy}\} + (s + 1)^{-1} \tag{4}$$

For a flange only one side of the stress field of Figure 1 is acting, but the width of that half is b instead of b/2. Then

$$\sigma_{xu}/\sigma_{cy} = s(s + 1)^{-1}\{b_e/b + [1 - b_e/b](1 - c)\sigma_{x\ cr}/\sigma_{cy}\} + (s + 1)^{-1} \tag{5}$$

In the preceding development it is assumed that the centerline stress in the plate remains at the critical value. This is open to question for a number of reasons. For wide plates, for example, the postbuckling stress may be near zero, as is explained below. For long plates, the centerline stress has been reported to decrease, by some investigators (Duffy and Allnut, for example, in Ref. 5), as the load is increased above critical toward ultimate. One of the most interesting results was obtained by C. Smith* during a test of a grillage under longitudinal compression. The plate postbuckling strains at the centerline decreased in the plates near one unloaded edge of the grillage, increased in the plates at the other edge, and remained essentially constant at σ_{cr} in the plates midway between. In that test the end loading was controlled by jacks to be uniform.

In the absence of more definitive data, the choice of constant postbuckling stress at the critical value has been made in developing the theory for perfect long plates longitudinally compressed.

Plate Buckling Theory

The fundamental mathematical theory of structural stability frequently utilizes a differential equation derived from the physics of the deformed state of the structure under load (see Appendix III). This equation can be solved to find the minimum magnitude of the type of load applied to the structure subject to the applicable boundary conditions.

Two tools of the theory are the stress-strain curve and the concept of critical strain. They are useful in analyzing inelastic buckling and assessing the influence of degrading factors. Exact mathematical solutions for both elastic and inelastic problems are available in closed form for a large number of shapes and boundary conditions. Numerical solutions have been obtained for cases which do not lead easily to closed-form solutions for which energy solutions (and, more recently, finite-element computer programs) are employed.

In the case of perfect rectangular plates the analyses yield the result

$$\sigma_{cr} = \eta[k\pi^2 E/12(1 - \nu_e^2)](t/b)^2 \qquad (6)$$

in which η embodies the inelastic properties of the plate material (Table II-1), while k embodies the effects of the boundary conditions and plate shape. For a simply supported infinitely long rectangular plate under longitudinal compression, k = 4 and (Table III-1)

$$\eta = \frac{1 - \nu_e^2}{1 - \nu^2}(E_s/E)[0.5 + 0.25(1 + 3E_t/E_s)^{1/2}] \qquad (7)$$

* Private communication

For the same plate under transverse compression, k = 1 and (Table III-1)

$$\eta = [(1 - \nu_e^2)/(1 - \nu^2)](E_s/E)[0.25 + 0.75(E_t/E_s)] \qquad (8)$$

Plasticity reduction factors for flanges are discussed below.

Strain Analysis of Plate Buckling

The principle of strain analysis is to seek the critical strain of a structure and then enter the stress-strain curve to find critical stress. For a perfect plate it requires prior knowledge of the value of η that applies to the problem. The method was used by Gerard to analyze plastic buckling of flanges (Ref. 6).

Suppose that the perfect-plate critical stress relation from Eq. (6) were to be written

$$\varepsilon_{cr} = \sigma_{cr}/E_{s\ cr} = [K(t/b)^2(1 - \nu_e^2)/(1 - \nu^2)](E_{s\ cr}/E)j \qquad (9)$$

where $K = k\pi^2/[12(1 - \nu_e^2)] = 0.905k$ at $\nu = 0.3$. Then

$$\varepsilon_{cr} = j[K(t/b)^2(1 - \nu_e^2)/(1 - \nu^2)] \qquad (10)$$

It is possible to use the stress-strain curve to chart ε_{cr} as a function of b/t for a given plate problem, and then to use the chart to enter the stress-strain curve in order to find σ_{cr}. This chart is shown schematically in Figure 2. The curve for the flange is parabolic in t/b except for the slight influence of Poisson's ratio. Also, comparative calculations show a difference of only a few percent between the values of j for a simply supported long plate and for a clamped long plate. There would be negligible error in critical stress if the simply supported plate j were to be used for both cases.

The critical-strain method of imperfect-plate buckling analysis is based on the principle that the perfect-plate critical strain is the sum of the strains due to residual stresses, to imperfections, to load variations, and to the mean uniform critical loading of the practical plate,

$$\varepsilon_{cr,p} = \varepsilon_r + \varepsilon_i + \varepsilon_v + \varepsilon_{cr} \qquad (11)$$

Consequently, ε_{cr} is found by subtracting ε_r, ε_i and ε_v from the critical strain of the perfect plate and then entering the stress-strain curve to find the critical stress of the imperfect plate, as shown schematically in Figure 3.

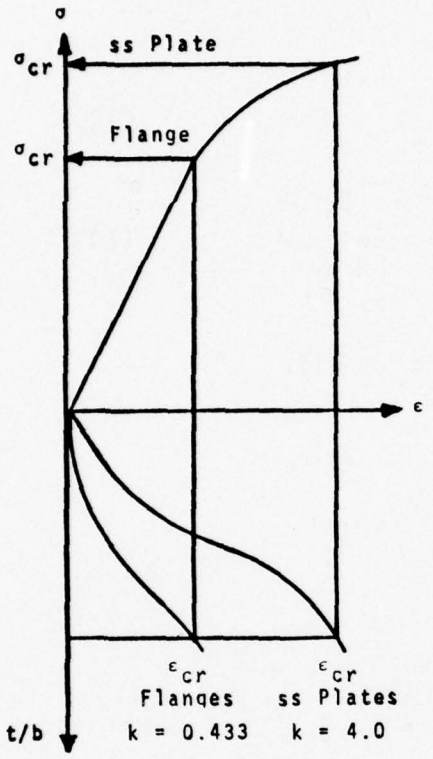

FIGURE 2
BUCKLING STRAIN ANALYSIS
FOR PERFECT PLATE

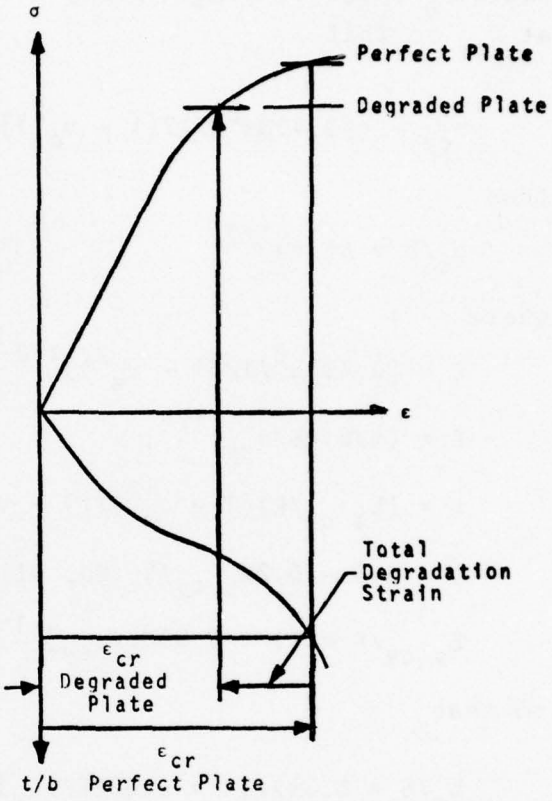

FIGURE 3
BUCKLING STRAIN ANALYSIS FOR
DEGRADED PLATE

Pseudo Flange Action

Each edge strip of the plate in Figure 1 is considered a flange of width b_e which is hinged along the unloaded edge and which buckles at σ_{cy} so that

$$\sigma_{cy} = \eta[0.433\pi^2 E/12(1 - \nu_e^2)](t/b_e)^2 \tag{12}$$

Then

$$b_e/b = CF(\eta)^{1/2} \tag{13}$$

where

$$C = [0.433\pi^2/12(1 - \nu_e^2)]^{1/2} = 0.626 \text{ with } \nu_e = 0.3,$$

$$F = (t/b)(E/\sigma_{cy})^{1/2},$$

$$\eta = (E_{s\ cy}/E)(1 - \nu_e^2)/(1 - \nu^2),$$

$$\nu = 0.5 - 0.2E_{s\ cy}/E \text{ (Eq. III-12)}$$

$$E_{s\ cy}/E = [1 + 0.002E/\sigma_{cy}]^{-1}$$

so that

$$b_e/b = 0.597F(1 + 0.002E/\sigma_{cy})^{-1/2} \times \{1 - [0.5 - 0.2(1 + 0.002E/\sigma_{cy})^{-1}]^2\}^{-1/2} = \beta F \tag{14}$$

Eq. (14) shows b_e/b to depend upon b/t and E/σ_{cy}. The range of $(b_e/b)/F$ is shown in Figure 4 over the range of E/σ_{cy} relevant to ship structural materials.

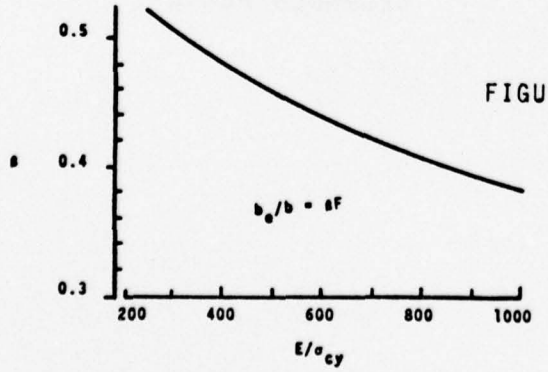

FIGURE 4 EFFECTIVE WIDTH OF PSEUDO FLANGES AT PLATE ULTIMATE LOAD

Theoretical Scatter Band

It was shown above that when supported plate degradation is so large as to obliterate the buckling stress then the ultimate load-carrying capacity will come only from the pseudo flanges and transition-curve stresses. In that case Eq. (2) becomes

$$\sigma_{xu}/\sigma_{cy} = (2sb_e/b + 1)/(s + 1) = (2s\beta F + 1)/(s + 1) \qquad (15)$$

For 1010 steel $E/\sigma_{cy} = 744$ (Table II-1) and $\beta = 0.417$ (Figure 4). Thus, at $s = 12$,

$$\sigma_{xu}/\sigma_{cy} = 0.77\ F + 0.077 \qquad (16)$$

For 4130 steel

$$\sigma_{xu}/\sigma_{cy} = 0.94\ F + 0.077 \qquad (17)$$

The bottom of the band is not the same for all materials. However, it reaches a limit of 0.077 for extremely thin plates for which $F \to 0$.

When the plate is thick, b_e/b approaches 1/2 and the bottom of the band will join the perfect-plate curve at $\sigma_{xu}/\sigma_{cy} = 1$. This will occur at

$$F = 1/2\beta \qquad (18)$$

which is 1.22 for 1010 steel and 0.98 for 4130 steel.

The band width is sensitive to σ_{cr}/σ_{cy}, as seen from

$$\Delta(\sigma_{xu}/\sigma_{cy}) = s(1 - 2\beta F)(\sigma_{cr}/\sigma_{cy})/(s + 1) \qquad (19)$$

It would be greatest for clamped square plates and least for long-hinged flanges. Maximization with respect to F shows that the band is thickest near the proportional limit (0.0001 offset strain). For extremely thin plates ($F \to 0$) the band width would be

$$\Delta(\sigma_{xu}/\sigma_{cy}) = s(\sigma_{cr}/\sigma_{cy})/(s + 1) \qquad (20)$$

which is 0.92 σ_{cr}/σ_{cy} at $s = 12$. The value of s was selected to fit the data at $1/F = 8$. If s were 8 or 16 it would alter the theoretical curve by only 2 percent when 1/F approaches 2.

General Discussion of Degrading Factors

Plate-strength degrading factors arise from all the processes to which a plate is subjected including fabrication in the mill, installation in the ship and the accumulated action of the sea upon the ship structure up to the moment of application of the load which would produce collapse by instability. An extensive bookkeeping process would be required, together with sophisticated measuring devices, in order to record that history of ship plate degradation. It is more practical to idealize the effects and to deal with probable ranges of the associated parameters.

The degrading factors most commonly mentioned in regard to plate strength are residual stresses and initial imperfections. An additional influence is the presence of stresses which cause a departure in the internal plate loading from the perfectly uniform stress field which normally is assumed to be applied to the plate. It is the purpose of this section, and of the three which follow, to discuss the manner in which those factors are taken into account in developing the theory presented in this report.

Degradation is assumed to be confined to the heart of the plate where the local load-carrying capacity of a perfect plate would be provided mainly by the critical stress. Therefore, reduction of the post-buckling load-carrying capacity would be equivalent to reduction of the critical stress for a long plate under longitudinal compression. Degradation is expressed as a fraction, c, of the critical stress. It is incorporated in the basic strength relation of Eq. (2)

$$\sigma_{xu}/\sigma_{cy} = s(s+1)^{-1}[2b_e/b + (1-2b_e/b)(1-c)\sigma_{cr}/\sigma_{cy}] + s(s+1)^{-1}$$

Degradation by Residual Stresses

Measurements have been made by various investigators (Refs. 7, 8 and 1, for example) to determine residual stresses in welding plates. The approach is to assume a stress field as shown in Figure 5. The problem is to determine representative values for the width of the tension block, which is usually expressed as a multiple, ℓ, of the plate thickness. The value of ℓ can range from 0 for an annealed laboratory test plate to a magnitude as great as 7 or 8 depending upon the welding procedure. There also has been some expression of the viewpoint that ℓ can be reduced by shakedown in a ship. However, there is a possibility that the reduction in ℓ may be converted to an initial imperfection (or to an enlargement of initial imperfections already present).

The force balance for the stress field in Figure 5 yields the relation

$$\sigma_r/\sigma_{cy} = (b/2\ell t - 1)^{-1} \qquad (21)$$

Once the value of ℓ is known for a plate with a given b/t fabricated from a material with a known σ_{cy} then the critical stress can be found from Eq. (21) and the strain, σ_r/E, can be found on the assumption that

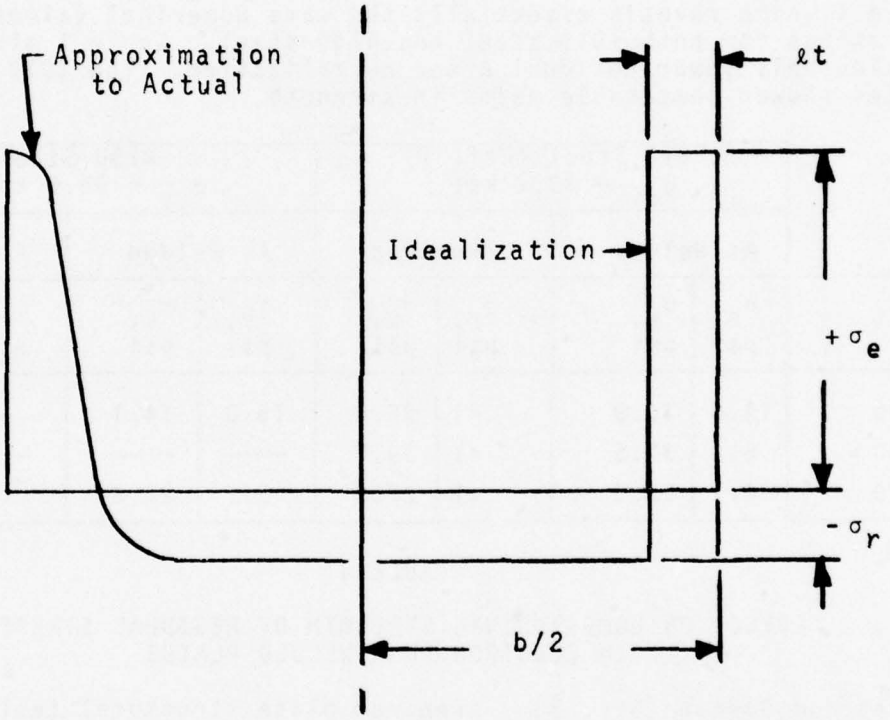

FIGURE 5 SIMPLIFIED RESIDUAL STRESS FIELD DEPICTING BALANCE OF INTERNAL FORCES

centerline residual is elastic.

The magnitude of ℓ has been expressed in terms of welding parameters (Ref. 8, for example). Those results have not been related to electron beam welding which was used in Ref. 1 and in the current tests. The residual stress fields for several plates were constructed through the use of a shaving operation described in Ref. (1). The centerline residual also was measured by trepanning, both in Ref. (1) and in a few specimens during the current study. The results show that the idealization of Figure 5 is not accurate enough for fine detailed analysis. However, it may be sufficiently accurate for practical use.

One of the interesting results of this investigation is shown in Table 1 which reveals essentially the same numerical values of residual stress for both 1010 steel and 4130 steel. Table 1 also shows a considerably lower residual after normalization. The 1010 and 4130 plates showed comparable gains in strength.

	1010 Steel (Ref. 1) σ_{cy} = 39.2 ksi				4130 Steel σ_{cy} = 98.6 ksi			
	As Welded		Annealed		As Welded		Annealed	
b/t	σ_r, psi	σ_u, psi	σ_r, psi	σ_u, psi	σ_r, psi	σ_u, psi	σ_r, psi	σ_u, psi
30	14.0	36.9	<1	36.8	15.0	54.1	<1	57.1
50	8.2	30.5	<1	33.7	———	———	———	———
70	4.7	20.3	<1	27.0	5.2	26.6	<1	30.1

TABLE 1

EFFECT ON LONGITUDINAL STRENGTH OF RESIDUAL STRESSES IN ELECTRON-BEAM WELDED PLATES

Dwight and Dorman (Ref. 9) prepared plate structural tests which included transverse welding as well as longitudinal welding. (They also included a variety of special imperfections typical of box-girder construction). The data agree well with Moxham's predictions when the transverse welds are well removed from the buckles. Ref. (9) should be consulted for practical design guidance since the purpose of the effort was to aid in establishing design rules for box girders.

Jubb et al (Ref. 10) explored plates with a variety of longitudinal and transverse welds in connection with natural frequency measurements to determine nondestructively the influence on longitudinal strength. They also have employed longitudinal centerline welding to recover plate strength lost by edge welding.

Duffy and Allnutt (Ref. 5) studied the influence of longitudinal and transverse internal welds on plates which were otherwise unwelded.

They showed a small gain in strength for longitudinal centerline welds and the same magnitude loss for transverse centerline welds.

If the welding residuals are large and the plate is thin then buckling may occur as a result of welding alone and the plate strength would be found on the bottom of the scatter band (c = 1). This would occur when $\sigma_r = \sigma_{cr}$ or, from Eqs. (6) and (21),

$$(b/2\ell t - 1)^{-1} = 3.62\ (E/\sigma_{cy})\ (t/b)^2 \qquad (22)$$

Table 2 shows the effect for 1010 and 4130 and indicates that high strength steel plates would suffer greater compressive strength degradation than the same size mild steel plates if the heat-affected zones are of equal width.

Material	b/t for ℓ = 3.5	ℓ = 7
1010 Steel	378	177
4130 Steel	148	59

TABLE 2

RELATION BETWEEN WELDING PARAMETER AND b/t FOR WELD-INDUCED BUCKLING

Degradation by Initial Imperfections

An initial imperfection is a geometric distortion from the flat state which exists in the plate before external membrane load is applied. It is often assumed that the magnitude of the distortion is significant only when the shape of the distortion matches the buckle pattern which the loading would be expected to induce. When load is applied in the plane of the hypothetically perfect plate the eccentricities of the load lines from the deflected median surface of the plate tend to amplify those imperfections. The amplification factors used by many investigators is that derived by Timoshenko (Ref. 11) for a variety of structures,

$$w/w_o = (1 - \sigma/\sigma_{cr})^{-1} \qquad (23)$$

It might be assumed that the initial imperfection would be amplified by an infinite amount as the applied stress approaches the critical value of the structure. It has been shown, however, (Refs. 1 and 5, for example) that the load-deflection pattern for a plate departs radically from the relation of Eq. 23 as the ultimate strength is approached, as shown in Figure 6.

The influences of the initial imperfections have to be considered in a variety of ways. For example, Timoshenko utilized Eq. (23) to identify the curvature of the center of the plate to which the stress (in com-

bination with the membrane stress) would reach the yield value at which point failure was assumed to occur. More recently, other theoretical approaches (discussed below) incorporate the behavior in the mathematics of post-buckling action.

Degradation by Internal Stress Deviations

It is shown below, in the section on experimental boundary conditions, that there is no practical method of conducting a plate experiment so that the boundary conditions are identical to those assumed theoretically in conducting plate-strength analyses. One of the potential degrading factors is the restraint, at the loading heads, of the Poisson lateral expansion under the longitudinal stress field. If the friction forces are large enough to permit complete restraint at those locations then a transverse compressive stress would be induced equal in magnitude to $\nu\sigma_x$. This laterally compressed zone might extend as much as 3/4 of the plate width away from each loaded edge. The effect would be to lower the level of the longitudinal stress at which buckling would occur. If loaded-edge rotational restraint is assumed to be absent, and if the interaction curve for an elastic biaxial stress field is employed, the longitudinal critical stress theoretically could be reduced by 40% or more.

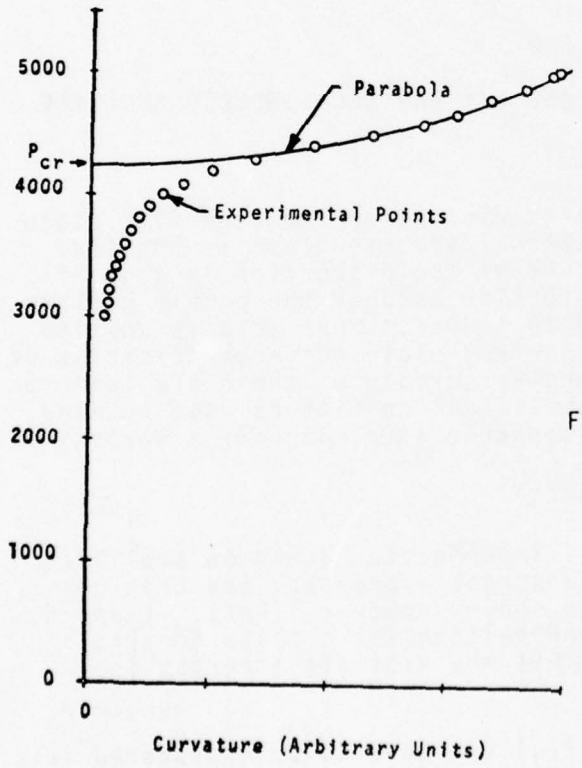

FIGURE 6 POST BUCKLING CURVATURE

Experimental Boundary Conditions

Theoretically, the process of buckling is considered to occur suddenly on a specimen to which the buckling boundary conditions are applied only at the onset of buckling and not before. Furthermore, the stress distribution is assumed to be controlled precisely to a prescribed distribution which is usually assumed to be uniform throughout the plate. An alternative assumption is that the end shortening is uniform at all load levels up to failure. It is virtually impossible to conduct a buckling experiment in complete consonance with the theoretical idealization because of the practical difficulty of achieving those conditions. The plates of these investigations were loaded in a manner that induced resistance to membrane strains, to transverse deflection and to twisting and bending at all load levels up to buckling. The prebuckling constraints induced prebuckling load nonuniformities in each specimen. Furthermore, the loading platens continued to exert restraints of the type just described during buckling, post buckling and failure. The precise measurement of those features would involve instrumentation considerably more extensive than the scope of this program permitted.

In spite of those effects, all specimens were assumed theoretically to be simply supported and uniformly loaded when a/b was equal to 3. It is doubtful that rotational restraint on the loaded edges was significant for specimens with a/b = 3 since the buckling stress for a clamped loaded boundary theoretically would be only 10 percent above the simply supported case for a/b = 3. The influence theoretically could have been much more for a/b = 1.5 and there is indication that this was true. Therefore, it would be necessary to assess the importance of this aspect of the testing process when checking correlation between theory and experiment, if the theory is based upon simply supported loaded boundaries.

There is no known method of specimen design and loading that avoids these problems completely. Every loading device includes some measure of uncertainty. In the NSRDC experiments (References 5 and 12, for example) the use of gripping structures along the unloaded edges may have affected the load distribution after buckling because of friction which could have caused some of the load to be carried in the grip columns. As a result, the plate failure stress could have been less than the apparent value from P_x/A_x. The primary virtue of square tube tests is the high probability that the specimen faces provide simple support to each other on the unloaded edges. Furthermore, it is reasonable to assume loading symmetry at any cross section of this specimen if the load boundaries have been fabricated with a high degree of flatness and if proper load distributing pads are used, as were done in these tests.

In addition to the rotational restraints possible at the loading heads, it is also possible for the membrane strains parallel to the loaded edges to be restrained by the loading heads as result of the friction between the head and loaded edge. This theoretically could induce a transverse membrane stress in the vicinity of the loaded edge as large as $\nu\sigma_x$. The consequent biaxiality would lower the longitudinal critical

stress of the plate in the region of the loaded edge and thereby reduce the plate strength as was discussed above. This effect also would occur where transverse frames or bulkheads are welded to the plate. In some measure, therefore, the test procedure of this investigation simulated the action of plates in a ship.

Effect of Plate Length

A portion of this investigation was devoted to an assessment of the effect of a/b on longitudinal strengths. This was stimulated by the observation of prevention of rotation on the loaded edges of all specimens which were tested in uniaxial longitudinal compression. It could not be determined (without extensive strain gaging beyond the scope of the current study)whether the rotational restraint equalled full clamping, however. The short-plate experiments were not conclusive since there was significant degradation initially, especially in the 4130 plates. Two actions were present. As the plates became shorter the longitudinal residuals would decrease while the effects of clamping also would enhance the strength. The remainder of the degradation action would have to be charged to imperfections and to transverse restraint.

	1010 Steel, Welded				4130 Steel			
		a/b				a/b =	a/b = 3	a/b = 3 Welded and
b/t	Theor.[1]	1.0	1.5	3	Theor.[1]	1.5	Welded	Annealed
30	0.98	.92 .93	—	—	0.97	0.88	0.55	0.58
50	0.94	.91	0.89	0.78	—	—	—	—
70	0.73	.66 .69 .71	0.65	0.52	0.46	0.47	0.27	0.31
90	0.53	.51	0.49	0.42	—	—	—	—

1 Figure 7

TABLE 3

EFFECT OF a/b ON LONGITUDINAL STRENGTH RATIO σ_{xu}/σ_{cy}

Part of the reason for the short-plate tests was to determine the feasibility of conducting biaxial strength tests on plates with a/b<3. (Transverse strength tests are discussed below). A study of aspects of the design of an appropriate loading fixture and test specimens revealed problems that could not be resolved during the investigation.

Theoretical Strength Curves for Simply Supported Plates From Eq. (2)

Figure 7 contains plots of the theoretical plate buckling and ultimate strengths for the two steels investigated in the current program. It is clear that the theory predicts one set of ultimate strength curves for each material stress-strain curve, which bears out von Karman's 40 year old prediction (Ref. 3). In addition, there are two buckling curves in the thick-plate region where plasticity influences the behavior.

For practical purposes, the two sets of curves of Figure 7 could function as bounds for a variety of steels and one may interpolate for a material for which the properties of the stress-strain curves are known.

The curves of Figure 7 pertain to long plates for which the influences of the loaded-end boundary conditions are assumed not to affect buckling and ultimate load-carrying capacity. If the plates are shorter, then those boundary conditions would begin to affect the curves. For example, rotational restraints would tend to raise the portion of each perfect plate curve in the intermediate and far elastic range which corresponds to I/F of the order of 3 or more.

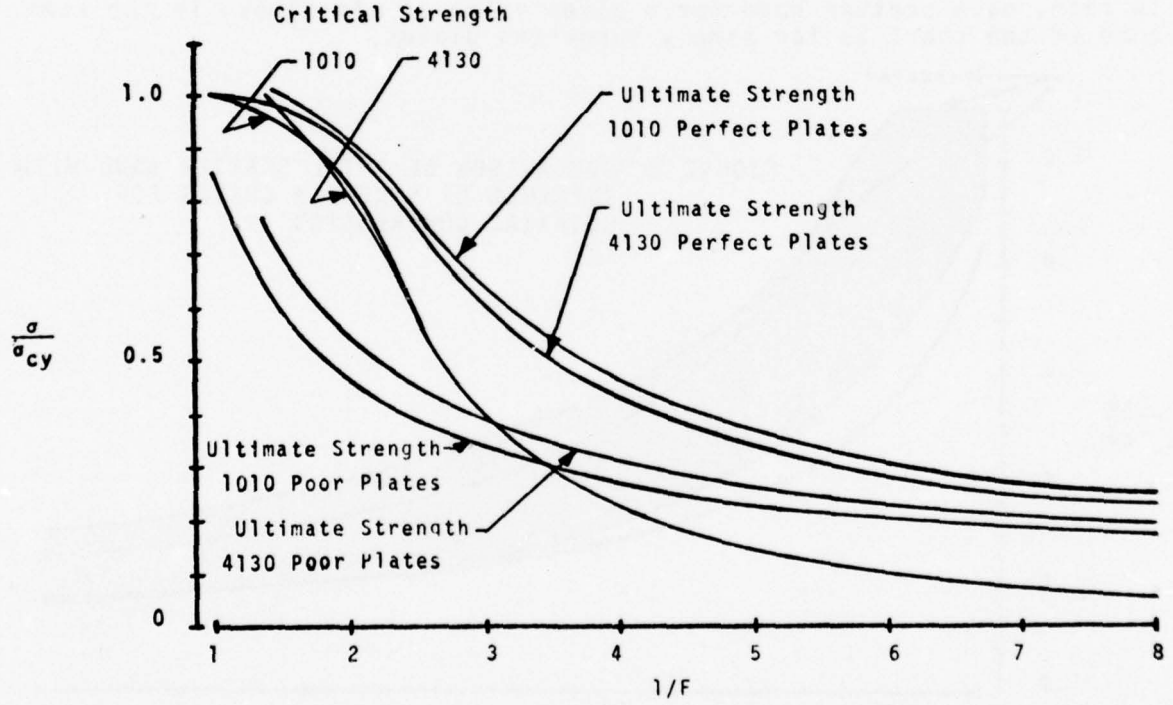

FIGURE 7 THEORETICAL BUCKLING AND ULTIMATE STRENGTHS OF SIMPLY SUPPORTED LONG RECTANGULAR PLATES UNDER LONGITUDINAL COMPRESSION

Comparison of Theory with Experiment

The experimental data embrace all the properties of the materials, a large part of the range of boundary conditions and plate proportions, and the gamut of plate degradation. An initial comparison has been made in Figure 8 by plotting the available data together with the extremes of the theoretical scatter bands shown in Figure 7. The general trend of the data in Figure 8 shows good agreement with the theoretical relations. It appears that the choice of s = 12 is appropriate. Furthermore, the nature of the scatter band at small F is reasonably well-defined and is shown to have the size indicated in Eq. (20). Some of the test points at small F are shown to have greater strength than the maximum value for a perfect plate. These may be the result of test restraints.

Figure 8 shows no relationship of data to degrading factors. This work was done by Moxham (Ref. 8) who tested plates with a large range of ℓ in fixtures which were designed to provide simple support or clamping to the plate boundaries. The comparison with the current theory is shown in Figures 9 and 10. The data band for simply supported plates shows upper bounds that are identified reasonably well by the theoretical curves for the selected values of ℓ. The clamped plate data do not appear to have attained the theoretical strength, however. In fact, each scatter band for a given value of ℓ is almost in the same zone of the chart as for simply supported plates.

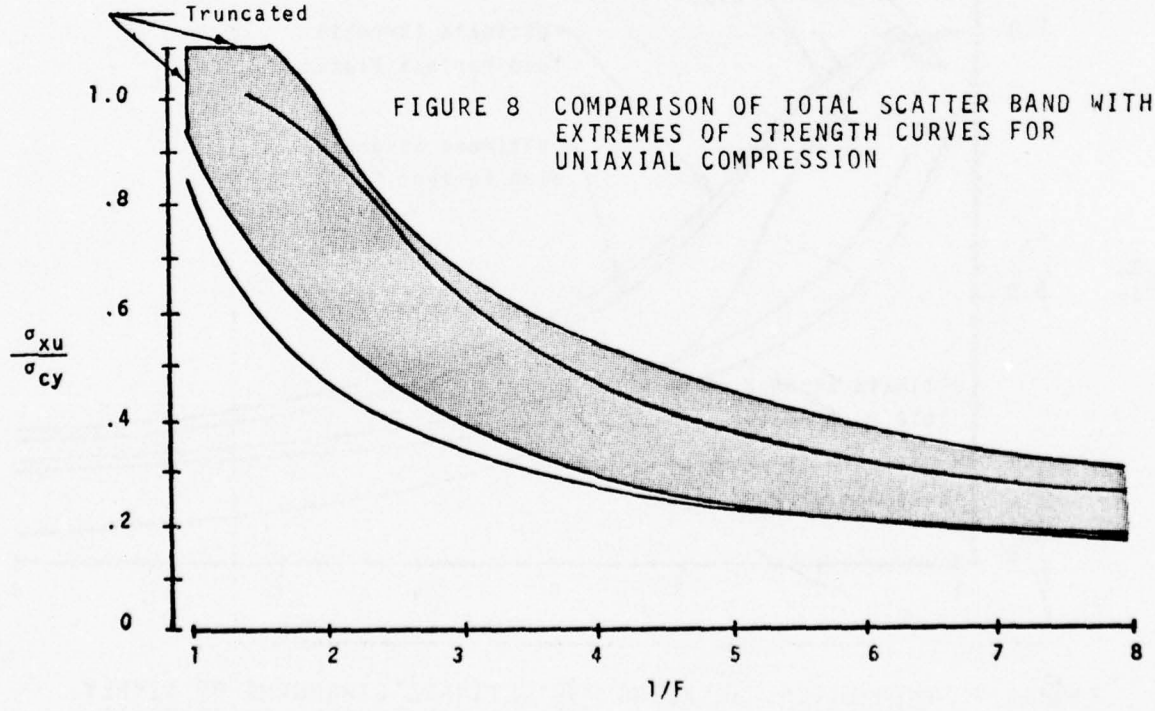

FIGURE 8 COMPARISON OF TOTAL SCATTER BAND WITH EXTREMES OF STRENGTH CURVES FOR UNIAXIAL COMPRESSION

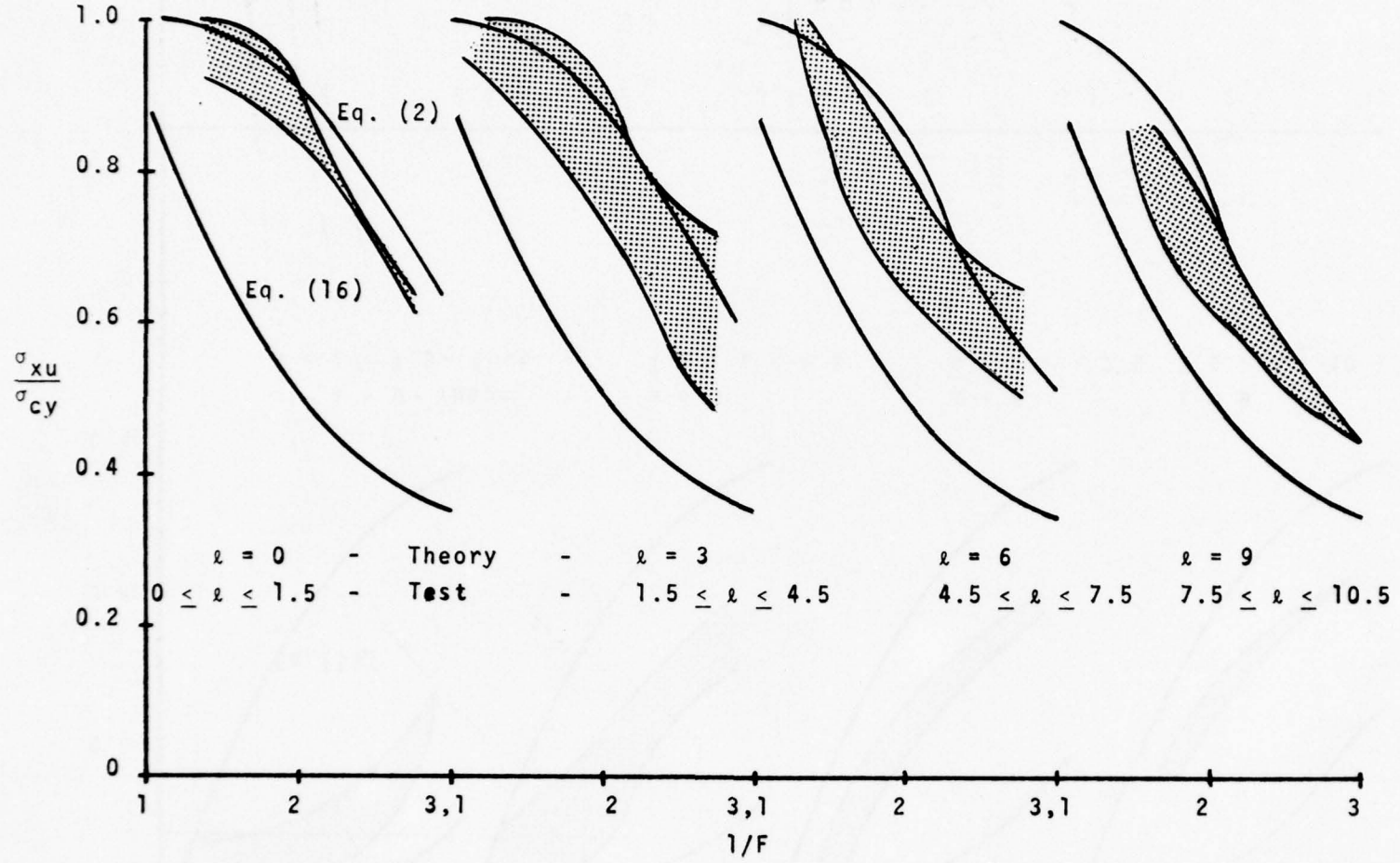

FIGURE 9 MOXHAM DATA FOR SIMPLY SUPPORTED PLATES (REF. 8)

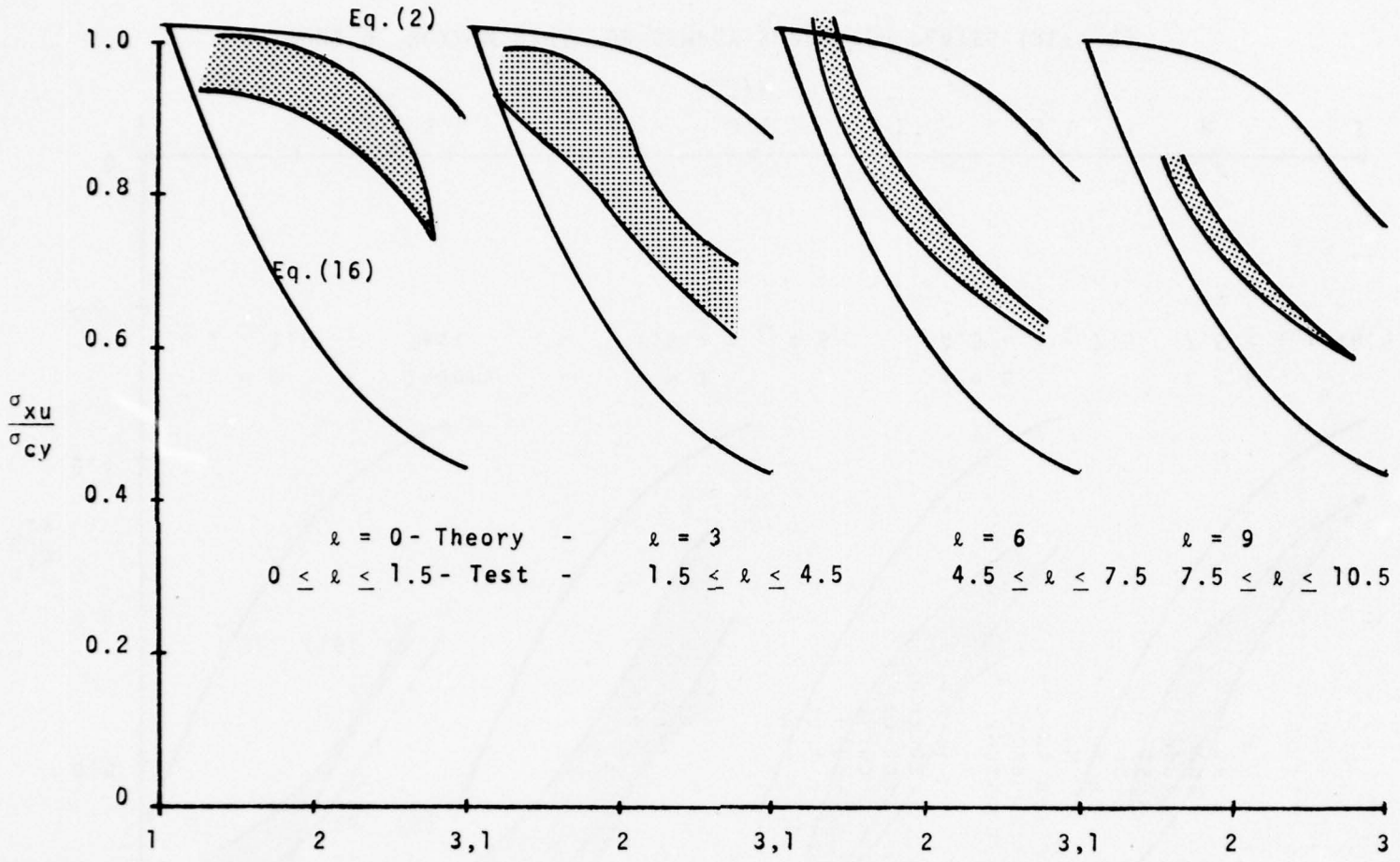

FIGURE 10 MOXHAM DATA FOR CLAMPED PLATES (REF 8)

Many of the test specimens in the scatter band of Figure 8 were fabricated into shapes such as angles and channels by bending a flat plate into the desired configuration. This could raise the compressive yield strength of the plate material in the bend zone thereby generating an increase in ultimate load-carrying capacity.

Figure 11 shows a comparison of data for high-strength steels with the theoretical curves for 4130, while Figure 12 shows a comparison of mild steels and aluminum alloys with the 1010 curves. Theoretically, it is improper to include the aluminum alloys in this comparision. However, many of those test specimens were formed by bending of initially flat plates into the desired shapes and the scatter band reveals the large gain in strength for the thicker plates which can occur as a result of that cold work. Material property data are not available to permit constructing the theoretical aluminum alloy curves to include that effect. Consequently, they have been included in Figure 12 only to reveal the magnitude of the achievable strength increase.

At this point it is possible to see the significance of the theoretical bounds of the scatter band. The general agreement with the test data show that no practical plate would be expected to have a strength less than the bottom curve. Also, perfect plates with simply supported edges probably would not exceed the strength level indicated by the top of the band. In fact, if a plate test should reveal higher strength it would be well to examine the details of that test guided by some of the factors mentioned above. It is important to indicate, in this regard, that Eq. (2) is not considered to be the most precise relation of plate strength. It agrees well with more basic theories, as discussed below; although there are differences. However, the important point is that any well-founded theoretical perfect plate curve will provide an upper bound from which departures may not be charged to variations in plate parameters alone.

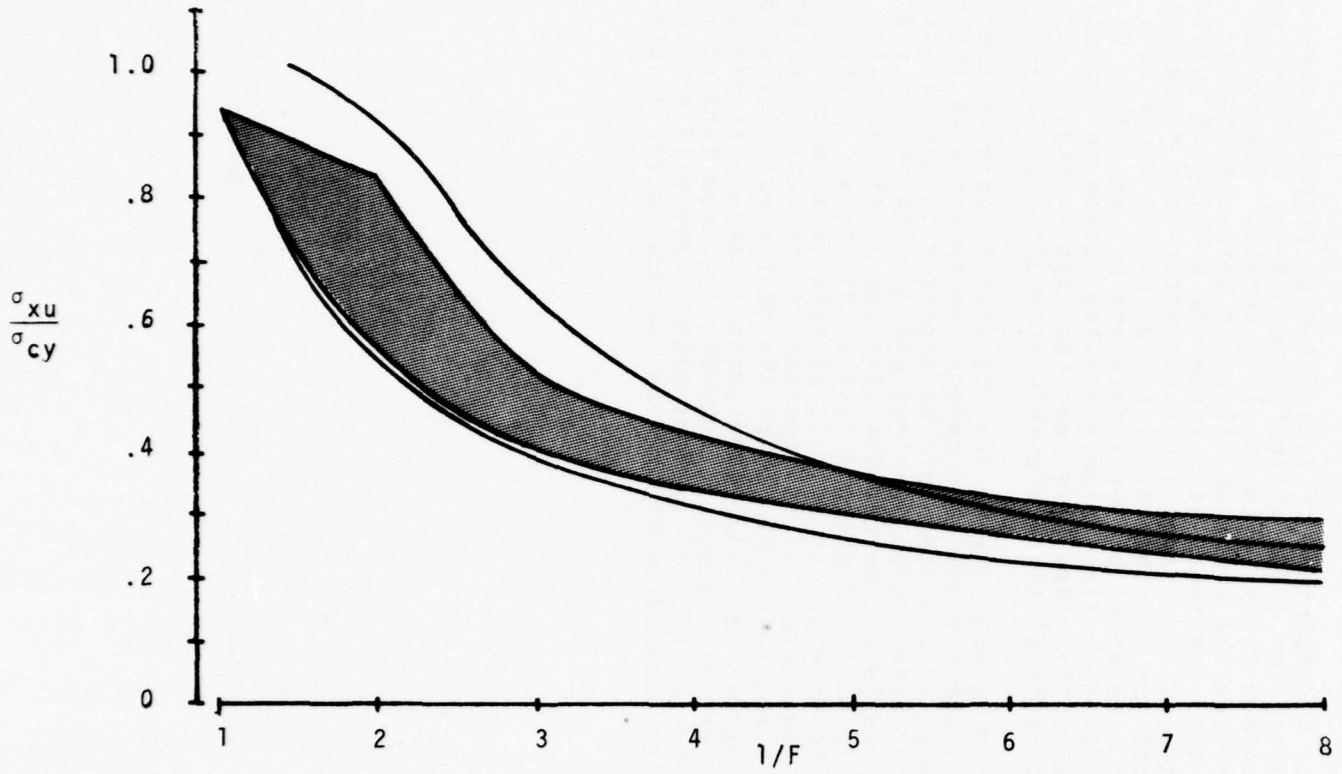

FIGURE 11 COMPARISON OF 4130 STEEL THEORETICAL LONGITUDINAL STRENGTH CURVES WITH HIGH-STRENGTH STEEL DATA

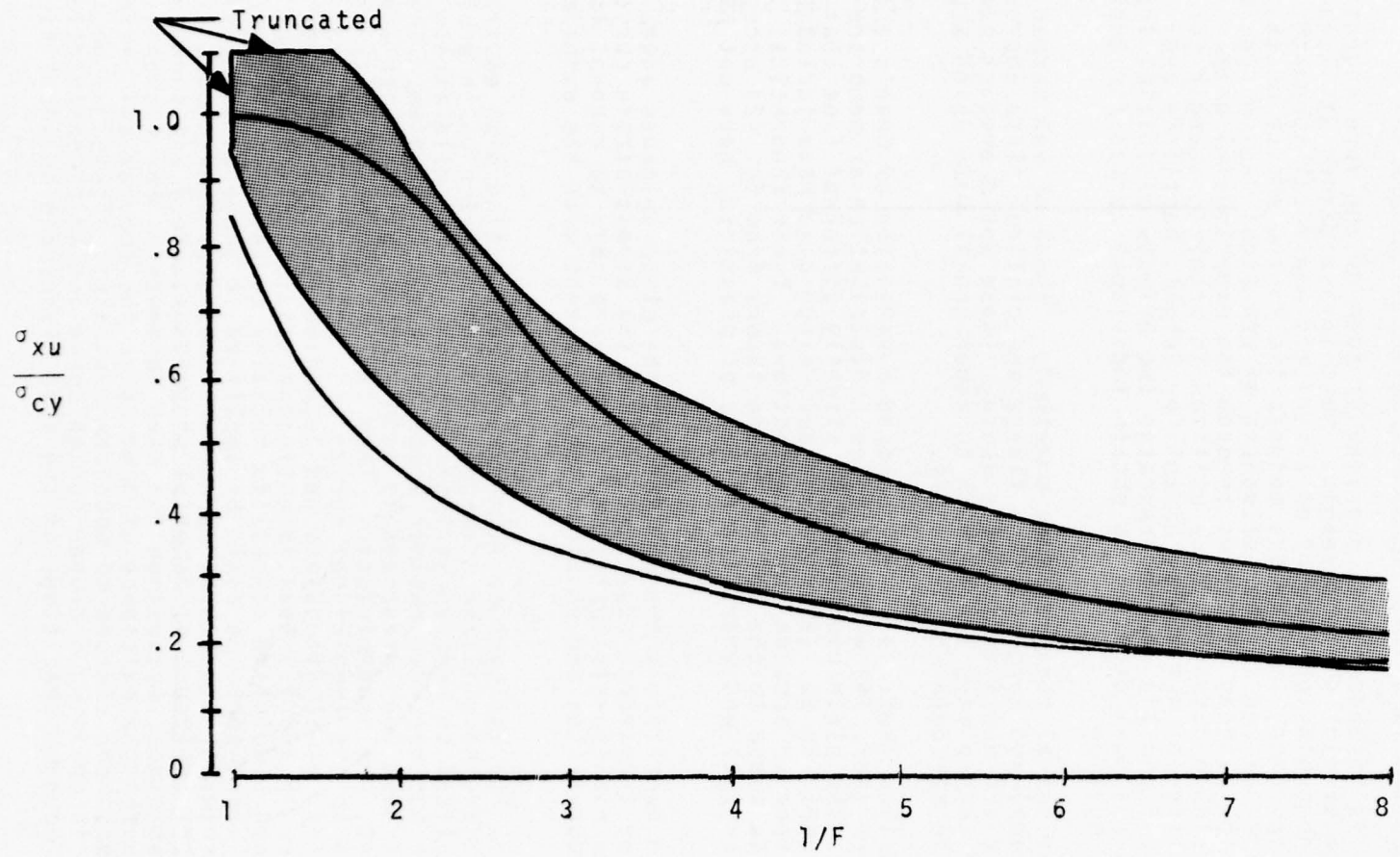

FIGURE 12 COMPARISON OF 1010 STEEL THEORETICAL LONGITUDINAL STRENGTH CURVES WITH MILD STEEL AND ALUMINIM DATA

Other Theoretical Procedures for Simply Supported Plates

This section is intended as an overview of some of the more recent approaches to predict plate strength. Most investigators utilized either a phenomenological theory or a strictly empirical approach. The differences among the various methods lie in the choice of the mathematical model and in the influences of practical design considerations upon the fitting of curves through the experimental data. In all cases a single curve has been utilized to predict strength for a variety of different materials, except for Dwight, Ractliffe and Moxham (Refs. 7 and 13) who incorporated the effects of initial imperfections and residual stresses to obtain individual curves for those types of degradation.

The phenomenological theories were essentially those of von Karman (the flange approach) and Bengtson (the flange and critical plate approach), both of which are mentioned briefly above. These would predict zero strength for thin plates in contrast to experimental data which appear to show finite strength for large b/t.

Dawson and Walker (Ref. 14) have employed a variation of Coan's theoretical procedure (Ref. 15) which utilizes a distribution of membrane stress across the plate width that is slightly different from that employed in deriving Eq. (2). Dawson and Walker also have included a degradation term to account for imperfections. Their theoretical curve (Figure 13) is close to the perfect plate theory from Eq. (2) except for the thick-plate end where the effects of plasticity have not been included.

In Dwight and Ractliffe's theory (Ref. 7) the plate unloaded edges were constrained by transverse edge stresses and the stress-strain curve was assumed to be elastic-elastoplastic. They were able to account for the effects of degradation and obtained good agreement with the experimental data.

Faulkner (Ref. 16) employed basic theory in conjunction with empirical curves. However, he utilized a tangent-modulus relation which would be highly specialized to tension stress-strain curves for mild steel. Faulkner also has explored another important strength problem. The theories that have been presented to date, including that which appears in this report, are deterministic. They include the possibility of modifications to the theoretical curves as a result of changes in material properties, plate dimensions and degrading factors. Faulkner and Mansour (Refs. 16 and 17) have investigated statistical approaches and have found good predictive capability relative to the mass of experimental data. That approach could be amplified in scope by addressing each of the relevant structural parameters (boundary conditions, types of degradation, influence of material properties, etc.) and then performing a statistical evaluation for each parameter. For example, some of the reason for the existence of data above the theoretical perfect plate curve has been charged to boundary restraint. These may be taken into account in defining a proper design curve for ship construction if the buckling boundary conditions of the ship plates can be identified.

Moxham (Ref. 8) calculated plate strength with a finite-element computerization based on the plastic variational principle in which residuals and imperfections are included. The analysis is based on an assumed elastic-plastic stress-strain curve (E_s/E = 1 for ε less ε_{cy} and 0 for $\varepsilon \geq \varepsilon_{cy}$). He compared strengths theoretically for a variety of values of ε_{cy}, E and b/t for each of several selected values of F. He found the same strength value over the total range of parameters at each F value and concluded that strength could be related to 1/F for all materials. This was in contradiction to the current result, and to von Karman's prognostication, that a different strength curve would be required for each of a range of materials with different stress-strain curves.

In order to test the concept more accurately in a fundamental way it would be necessary to utilize the complete stress-strain curve in the yield region. It is doubtful that an elastic-elastoplastic curve ($E > 0$ at $\varepsilon \geq \varepsilon_{cy}$) would be sufficiently accurate.

One of the interesting results of Moxham's analysis was the indication that the ultimate strength of a plate could be attained with the ultimate amplitude of an imperfection of the order of the plate thickness at the instant of failure. This differs from the value, used by Dawson and Walker, of an ultimate imperfection equal to 4t. However, Moxham also showed little variation in ultimate strength for a large range of initial imperfections and ultimate imperfections, both theoretically and experimentally.

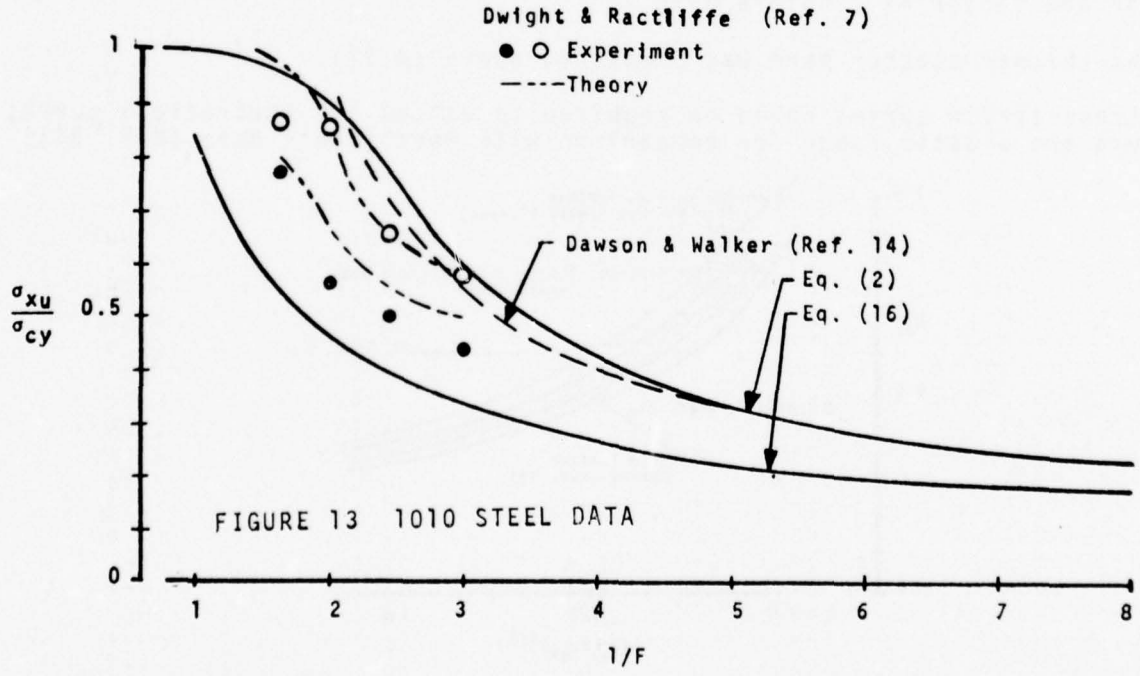

FIGURE 13 1010 STEEL DATA

Flange Strength

The general utility of the basic plate strength concept was tested by comparing the predictions to flange test data. The internal stress diagram of Figure 1 leads to Eq. (5)

$$\sigma_{xu}/\sigma_{cy} = s(s + 1)^{-1}[b_e/b + (1 - b_e/b)(1 - c)\sigma_{cr}/\sigma_{cy}] + (s + 1)^{-1} \qquad (5)$$

Stowell developed a basic theory of flange strength (Ref. 18). It agrees with test data only at small values of F, which is proportional to $(\sigma_{cy}/\sigma_{cr})^{1/2}$. A comparison was made in Ref. 19 using test data on cruciforms and formed angles. The results are presented in Figure 14 together with Stowell's theory and also with Eq. (5). The theoretical bottom of the scatter band also is shown. It was obtained by letting c = 1 in Eq. (5), which yields

$$\sigma_{xu}/\sigma_{cy} = (sb_e/b + 1)/(s + 1) \qquad (23)$$

This, also, is the same as for supported plates [Eq. (15)] except for the factor of 2 before b_e/b.

The thinner scatter band was predicted above (p.17).

Stress-strain curves would be required to extend the theoretical curves into the plastic range for comparison with Ractliffe's data (Ref. 24).

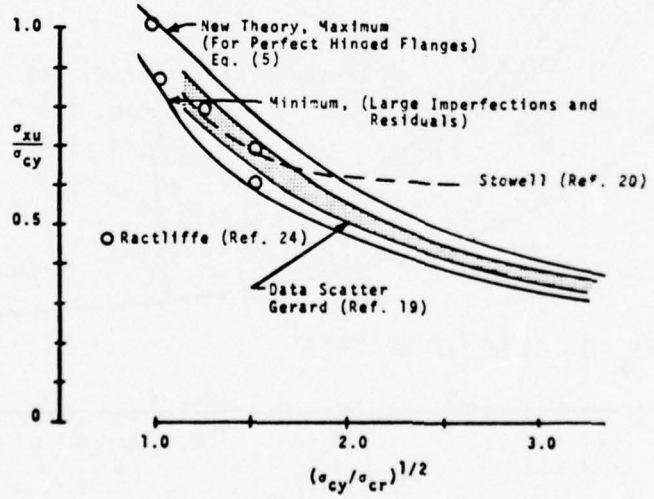

FIGURE 14 FLANGE STRENGTH COMPARISONS

UNIAXIAL TRANSVERSE STRENGTH

Introduction

The prediction of transverse strength is discussed in the following paragraphs primarily to identify the aspect of the strength degrading factor, which is slightly different in form from that which affects longitudinally compressed plates.

Eq. (4) can be used to predict the strength of a transversely compressed plate with $a/b > 1$. One of the problems in predicting transverse strength is associated with the determination of the postbuckling stress at the heart of the plate. In an extremely long plate the transverse loading would tend to induce wide-column action. A column is known to exhibit negligible postbuckling load-carrying capacity. For a square plate the postbuckling load would be the same as for a long plate compressed longitudinally. Consequently it is necessary to define the transition of the postbuckling action for $1 < a/b < \infty$. This may be viewed as an additional degrading factor.

Postbuckling Stress Distribution

The postcritical stress at the heart of a transversely compressed plate might be expected to approach zero for a perfect long plate under transverse compression, to be equal to the critical stress (for a perfect plate) when $a/b = 1$, to decrease gradually at first as a/b is increased from 1, and to approach the zero value asymptotically. There is no information in the literature on this phenomenon. Furthermore, a basic mathematical solution of the problem was not attempted at the present time. It is an area for further research. The approach taken in this project was to assume a variation as shown in Figure 15. The coefficient α is expressed in the form

$$\alpha = [(a/b - 1)^2 + 1]^{-1} \tag{24}$$

It is a multiplier of σ_{cr}/σ_{cy} in Eq. (4) which now will take the form

$$\sigma_{yu}/\sigma_{cy} = s(s + 1)^{-1}\{2(b_e/b)(b/a) + [1 - (2b_e/b)(b/a)(1 - c)\alpha(\sigma_{cr}/\sigma_{cy})]\} + (s + 1)^{-1} \tag{25}$$

Effect of Residual Stresses

When a plate is welded on all four edges, residual stresses are induced both longitudinally and transversely. If the two effects are assumed to be separable and superposible, then the transverse component at the longitudinal centerline in the midlength would be predictable in the same manner as for the longitudinal residuals. However, if the plate is long, then it is unlikely that the residual stress field will extend far from the short welded edges. It

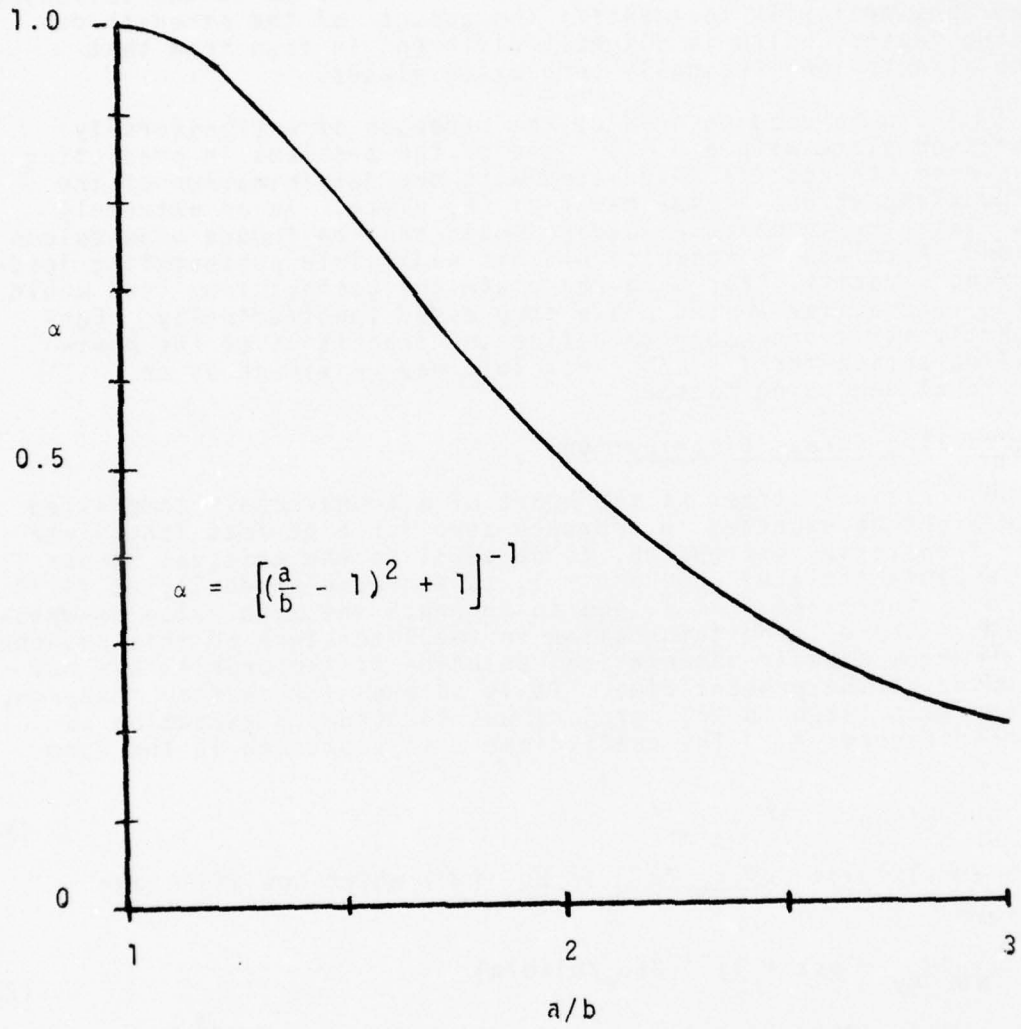

FIGURE 15 TRANSVERSE POSTBUCKLING EFFECTIVENESS AT CENTER OF LONG PLATES

probably would be confined to a region that would extend lengthwise no further than three-quarters of one plate width. In effect, the behavior would be synonymous to flange action. On the assumption that pseudo flange width equals 3b/4, the residual transverse compression (on the assumption of rectangular and compression blocks)is

$$\sigma_r/\sigma_{cy} = (3b/4\ell t - 1)^{-1}. \quad (26)$$

The effect of this residual stress distribution is to decrease the strength in a zone not far from a loaded edge but to leave it unaffected in the middle of the plate.

Effect of Initial Imperfections

The critical imperfection shape for a transversely compressed long plate would be a transverse half wave which extends essentially the full length of the plate. This is different in form from the critical imperfection shape for longitudinal compression which would be pillow-shaped with a square periodicity. Therefore, it would be unlikely that a long plate would be degraded simultaneously by a single imperfection. In fact, if the initial imperfection were to match the longitudinal buckle pattern then the transverse buckling stress might be enhanced. However, the influence on strength may differ from the influence on buckling stress because the failure mode shape would be a single buckle both longitudinally and transversely.

Stress Non-uniformity

If a plate were to be compressed transversely, the lengthwise Poisson expansion could be resisted thereby inducing a biaxial field in a manner which is the reciprocal of the effect induced by longitudinal loading. In a laboratory test the frictional constraints would induce an action of this nature unless steps were taken to permit free longitudinal motion. In the current series of experiments the use of a whiffletree avoided this problem. However, it also caused a departure from the behavior of a plate in a ship in which the longitudinal stiffening system would induce such a constraint. It would be effective to a small degree, however, since the stiffener cross-section area might be considerably less than that of the plate or (at a maximum) of the same magnitude as that of the plate.

Effect of Plate Length

Transverse strength tests were conducted on 4130 plates with a/b = 1.5. The strengths were calculated using Eq. (25). For b/t = 30, σ_{yu}/σ_{cy} = 0.55 compared to the theoretical value of 0.71 while, for b/t = 70, σ_{yu}/σ_{cy} = 0.31 compared to 0.31 theoretically. As in the case of the short longitudinal tests the results are not conclusive. Imperfections were still present while longitudinal residuals probably were reduced. There should have been no clamping action. However, some transverse membrane stresses should have remained as a result of the welding to the end plates.

BIAXIAL STRENGTH

Introduction

The phenomenological uniaxial strength theory has been enunciated and experimental support has been delineated. The primary physical mechanism of plate strength is the attainment of the compressive yield strength at the plate supported edges. In the uniaxial case, those were the edges parallel to the loading direction. The yield strength would be the value obtained from a uniaxial stress-strain curve.

In this section a theory is presented for biaxial strength based upon the same general type of physical behavior as for uniaxial strength. The only difference is the utilization of a law of yielding for biaxial fields. In the case of biaxial compression all four plate edges are under load. It is possible for failure to occur at either pair of plate edges. Therefore, it would be necessary to determine which set of edges reaches combined-stress yield first. In general, this determination can be made beforehand for a range of a/b and charts can be constructed to identify plate strength. Charts are included in this report for a/b = 3 to compare theory with experiment.

The theory embraces the range from thick plates (for which plastic-buckling behavior controls) to very thin plates (in which the buckling stress is an extremely small proportion of the maximum load-carrying capability).

The theoretical approach has two aspects. One involves the identification of the numerical loading combination for a specific plate from which it is possible to compute σ_{cu}. In the other, nondimensional relations are presented for determining interaction under biaxial loading.

Upon completion of the presentation of the basic theory, the experimental data from the current test series and from Ref. 1 are employed to depict the correlation with theory.

Principle

As stated above, the biaxial-strength theory for plates is based on the principle that the load-carrying capacity will be reached when the stress field at any edge satisfies the plasticity condition (Ref. 20)

$$\sigma_{cy}^2 = \sigma_x^2 + \sigma_y^2 - \sigma_x\sigma_y \tag{27}$$

For inelastic buckling, the ultimate load is assumed to be synonymous with the critical load and plastic-buckling theory is directly applicable. Furthermore, Eq. (27) is germane to inelastic-buckling theory as shown in Appendix II.

Theory

The postbuckling stress field in a biaxially compressed rectangular plate that buckles elastically is assumed as shown in Figure 16. This model is an extension of the uniaxial phenomenological model. The difference is the set of biaxial fields in the edge regions.

It is possible to deduce a general aspect of biaxial strength from the model in Figure 16. If the postbuckling stresses at the plate center were to be considerably less than σ_{cy}, then the edge stress could approach σ_{cy} in either the x or the y direction. This means that there would be little interaction between the strengths for any load combination.

The basic theoretical procedure employs Eqs. (2) and (25) for longitudinal and transverse strengths, respectively,

$$\sigma_{xu}/\sigma_{cy} = s(s + 1)^{-1}\{2b_e/b + (1 - 2b_e/b)(1 - c)\sigma_{cr}/\sigma_{cy}\} + (s + 1)^{-1} \quad (2)$$

$$\sigma_{yu}/\sigma_{cy} = s(s + 1)^{-1}\{2(b_e/b)b/a + \alpha[1 - 2(b_e/b)b/a](1 - c)\sigma_{y\ cr}/\sigma_{cy}\} + (s + 1)^{-1} \quad (25)$$

For a given load combination the edge stresses are computed using the plasticity condition of Eq. (27). However, no change in effective width is assumed. This theoretically should involve little error since there should be 15 percent deviation at the most in the edge values of σ_x or σ_y at failure according to Eq. (27).

The application of the theory requires knowledge of the biaxial postbuckling x and y stresses at the heart of the plate. This, in turn, requires data on the effect of residual stresses, initial imperfections, constraint stresses and the influence of normal pressure. Another aspect of biaxial strength is the process of mode jumping in which a plate in biaxial compression will buckle in one mode (possibly 3 half waves longitudinally for a/b = 3) and fail in another (one half wave longitudinally) as was observed during the experiments of Reference 1. This implies one set of stresses in the heart of the plate between buckling and failure and another stress field at failure. Also, the behavior would depend upon whether the test load is a uniform distribution of membrane force (which was employed in the current studies) or a uniform membrane displacement.

These complexities were bypassed in the current study by utilizing normalized interaction relations (See Figures 17-21) to see if the elastic buckling interaction curve would be usable for thick plates, in which plastic buckling would occur, and to see if the stress intensity relation would apply to thin plates, in which buckling would be elastic. This was attempted in Reference 1 without success. However, the uniaxial

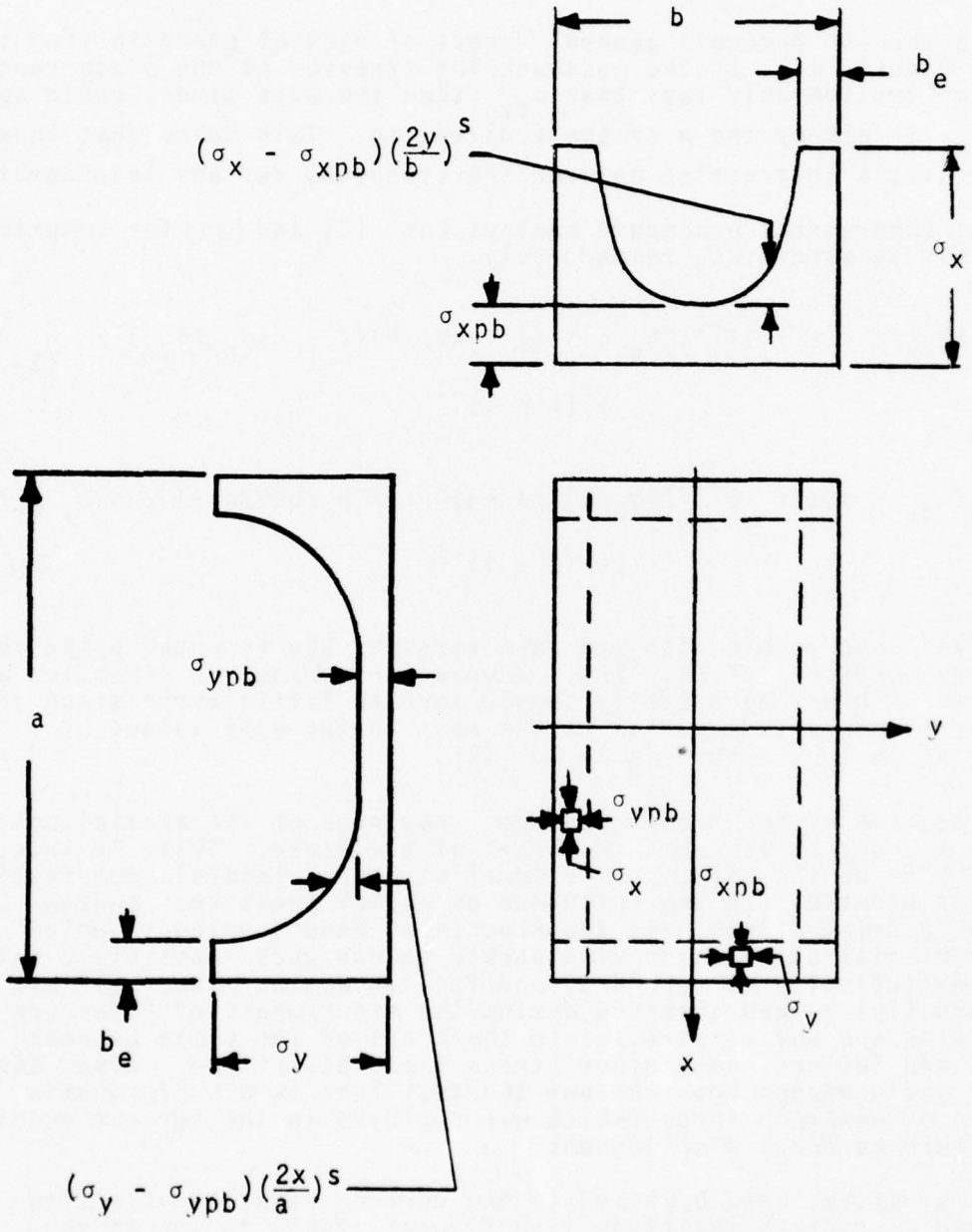

FIGURE 16 BIAXIAL POSTBUCKLING STRESS DISTRIBUTION

transverse strengths were not correctly determined in that study because of improper boundary conditions. More reliable values were employed in the current task based on uniaxial transverse strength theory and on measured transverse strengths using end plates to enforce simple support at the tube ends when $\sigma_x = 0$.

In summary, then, the approach to biaxial ultimate strength determination in this investigation was to utilize uniaxial strength data and then to employ interaction relations in terms of the stress ratios σ_x/σ_{xu} and σ_y/σ_{yu}. In order to apply this procedure properly to biaxial strength prediction it is necessary to have a complete background of data on uniaxial longitudinal and transverse strengths to be able to compute σ_{xu} and σ_{yu} for practical plates.

Comparison of Theory with Experiment

Figures 17 through 21 display the biaxial test results for 1010 and 4130 steels. The reference ultimate strength for the 1010 steel transverse stress ratio ($R_y = \sigma_y/\sigma_{yu}$) was the theoretical value. The experimental value of σ_{xu} was used for the longitudinal compression stress ratio ($R_x = \sigma_x/\sigma_{xu}$). The circles on the R_y axes of Figures 17 through 20 depict the observed transverse strength for 1010 steels, in which improper boundary conditions were employed.

In the construction of Figure 21 the experimental transverse strengths were used together with the experimental longitudinal strengths for both stress ratios.

The general trend of the data for biaxial strength alone is seen to vary from the elastic interaction relation for b/t = 30 to the plastic stress intensity relationship Eq. (27) for b/t = 70 in the carbon steel specimens. At b/t = 30 both the longitudinal and the transverse compression strengths approached yield. They were elastic at b/t = 90.

For 4130 steel the results appear to support the use of the stress intensity interaction law except for the welded plates with b/t = 30. The reason for the large values of R_y on those specimens is not clear. They may have been less degraded than the other 4130 specimens. It is to be noted that the uniaxial longitudinal strengths were observed to lie close to the bottom of the theoretical 4130 scatter band for the test specimens, for which b/t = 30 and 70.

The effect of normal pressure is not easily identifiable. In a few cases the pressure did not appear to change the position of the test point on the interaction diagram while, for other specimens, the strengths appeared to have been shifted from the stress intensity law to the elastic biaxial buckling interaction law. It would have required a considerable increase in the scope of the project to test enough specimens at appropriate pressures to identify the trend of biaxial strength for selected stress ratios. A discussion of the relationship of normal pressure to biaxial strength appears below.

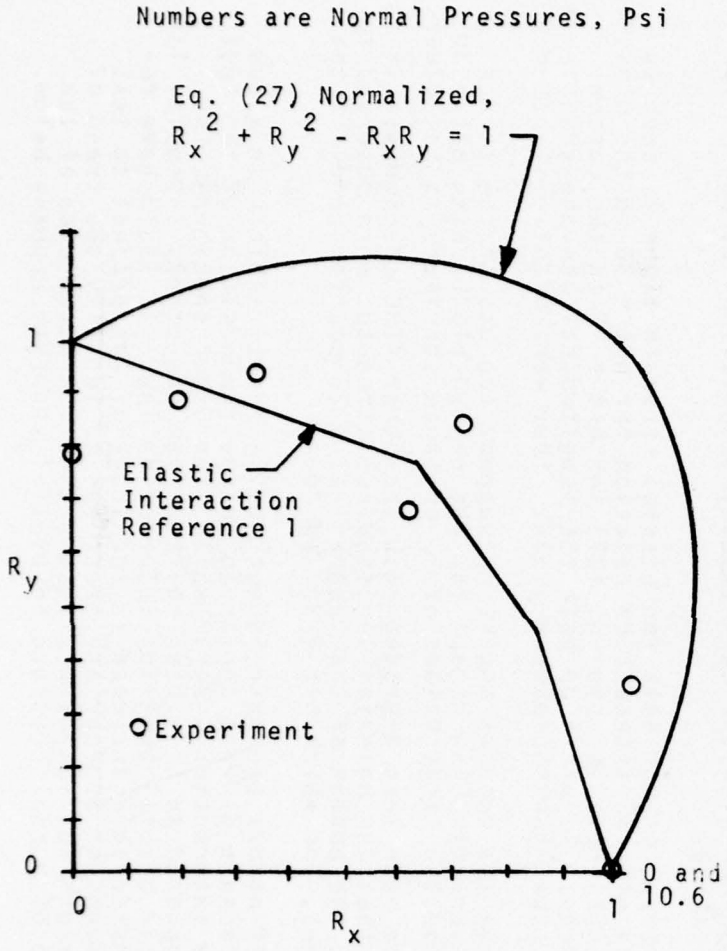

FIGURE 17 BIAXIAL STRENGTH COMPARISON, 1010 STEEL, b/t = 30

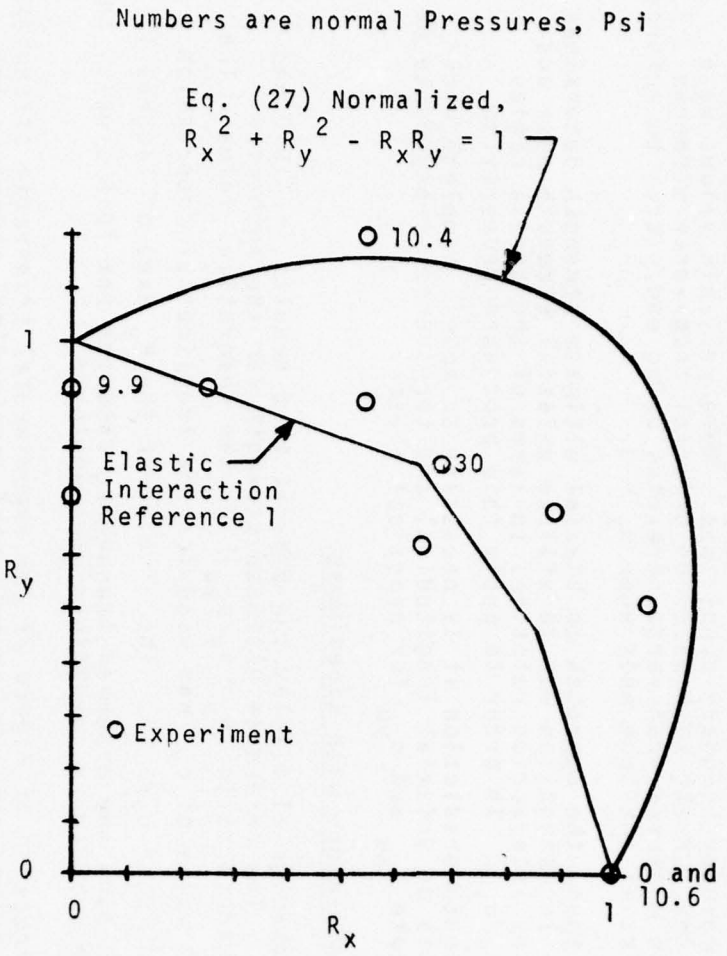

FIGURE 18 BIAXIAL STRENGTH COMPARISON, 1010 STEEL, b/t = 50

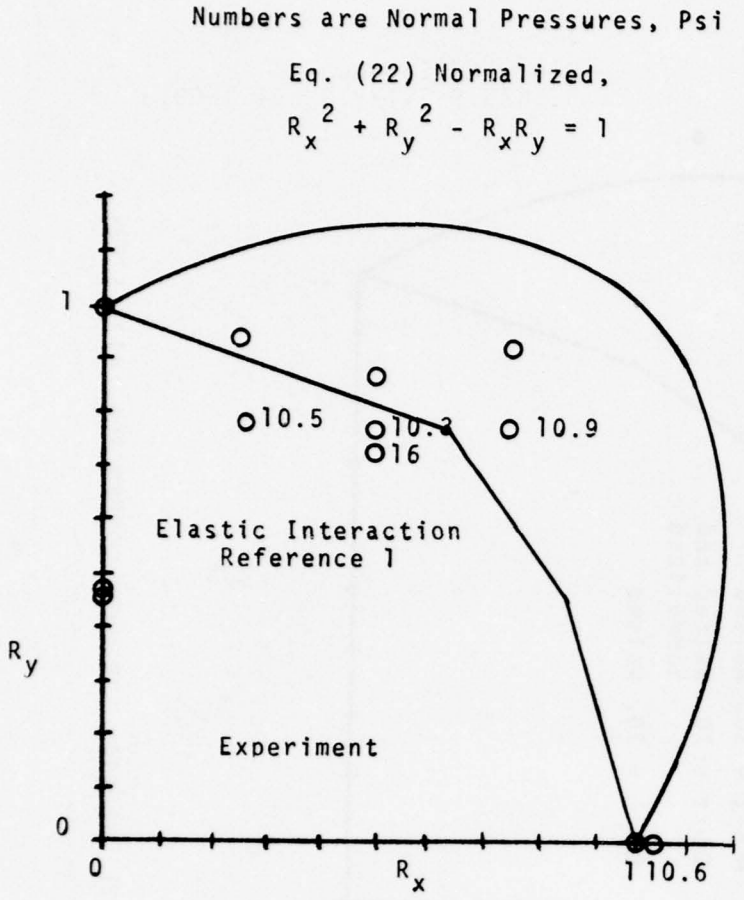

FIGURE 19 BIAXIAL STRENGTH COMPARISON, 1010 STEEL

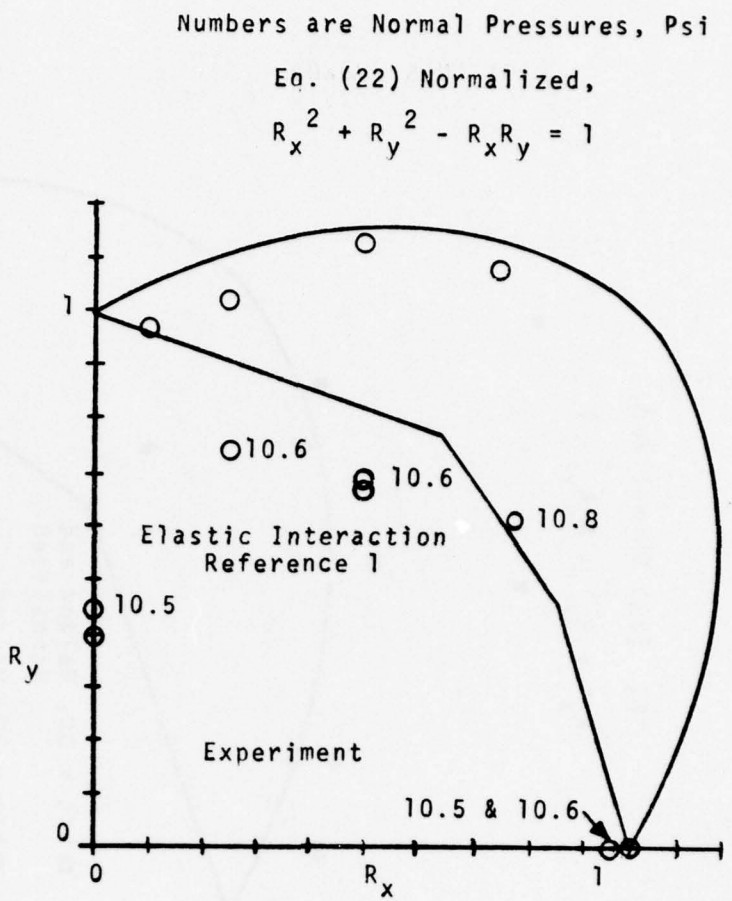

FIGURE 20 BIAXIAL STRENGTH COMPARISON, 1010 STEEL

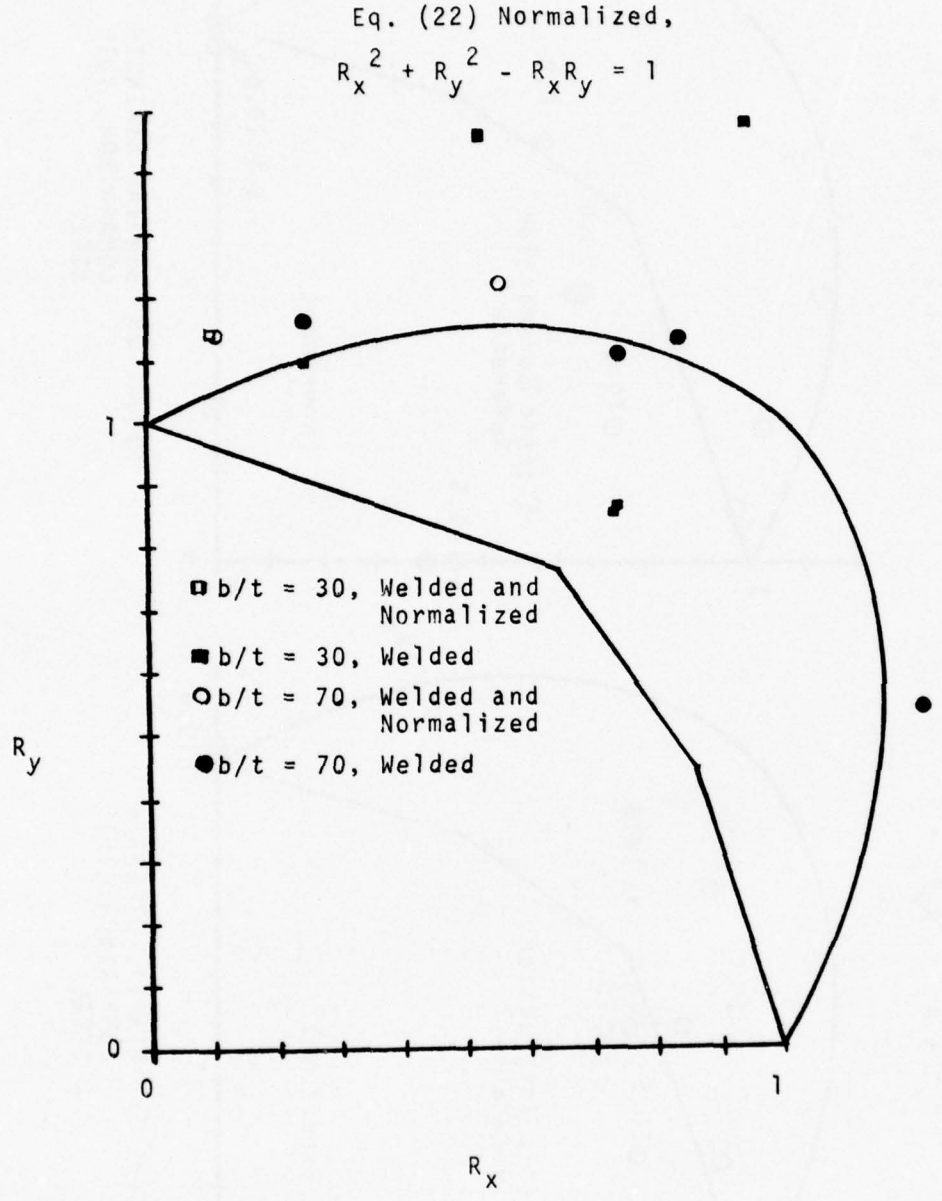

FIGURE 21 BIAXIAL STRENGTH COMPARISON, 4130 STEEL

EFFECT OF NORMAL PRESSURE

Longitudinal Strength

The application of normal pressure to a perfect plate would tend to bulge the plate into an initial imperfection, the shape of which would depend upon the plate boundary conditions. If the plate were simply supported then the application of normal pressure to a long plate would tend to deform the median surface of the plate into a sector of a cylinder with a cross-section shape approaching parabolic. The cylindrical shape would be constant except near the ends where the deflection would be maintained at zero.

If the plate were to be subjected to longitudinal compression the cylindrical shape would stiffen the plate against buckling, which would occur as a continuous sine wave in a long flat plate. The consequent gain in buckling strength was investigated by Levy and his coworkers (Ref. 21) through the use of large-deflection theory. A simple approximation was developed in Ref. 2 based upon the hypothesis that the plate would behave as a section of a cylinder in compression. This predicts much smaller strengths than the Levy approach. However, it agrees reasonably well with the trend of the experimental data shown in Table 4.

	1010 Steel p = 10 psi		4130 Steel p = 30 psi	
b/t	Theory	Exper.	Theory	Exper.
30	<0.01	<0.01	<0.01	0.06
50	<0.01	<0.01	—	—
70	0.04	0.06	0.10	0.12
90	0.26	-0.03	—	—

TABLE 4

LONGITUDINAL STRENGTH INCREASE, $\Delta(\sigma_{xu}/\sigma_{cy})$, DUE TO NORMAL PRESSURE

The cylindrical shell theory requires the calculation of the central radius of curvature of the cylindrical bulge. This can be done using elementary beam theory. When the result is combined with the chart that relates cylinder compression strength to shell geometry (Ref. 22), which is duplicated in Figure 22, the buckling strength relative to a flat plate can be computed with the relation

$$\sigma_{cr}/\sigma_{cr\ flat} = 1 + 0.027\ (Cp/E)^2\ (b/t)^8 \qquad (26)$$

This approach is an approximation. It is subject to significant error because of the fact that thin-wall cylinder strength prediction has a low degree of reliability (Ref. 22). This sensitivity is reflected in a range of values for C at any given value of $(p/E)(b/t)^2$. The curve in Figure 22 is an average.

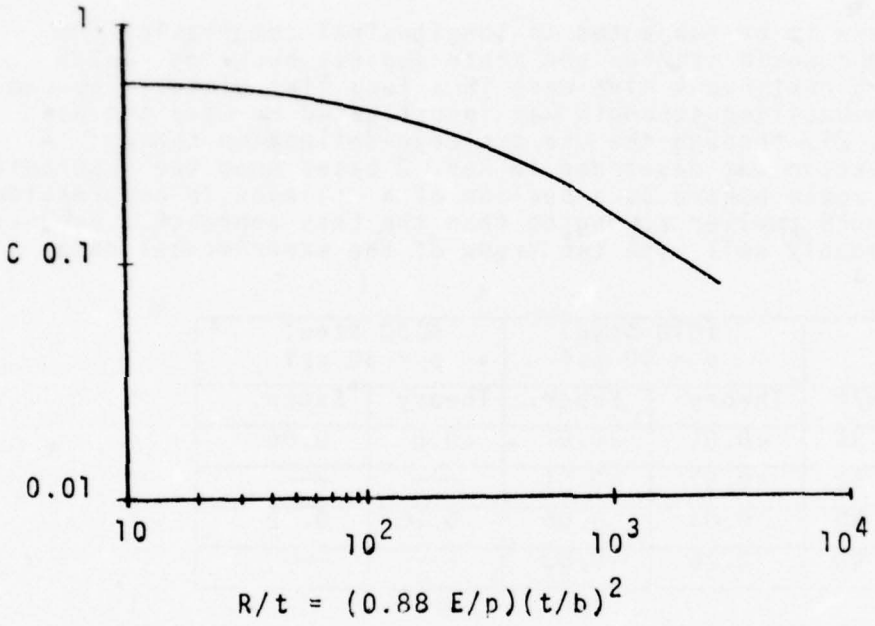

FIGURE 22 BUCKLING COEFFICIENT FOR NORMAL PRESSURE EFFECT, EQ. (26)

The increase in longitudinal buckling strength should lead to a corresponding increase in longitudinal ultimate strength if the post-buckling stresses at the heart of the plate were to remain at the enhanced value induced by the normal pressure. The data in Table 4 would appear to support that hypothesis.

Transverse Strength

The same deformation shape that enhances longitudinal strength, as a result of normal pressure application, would tend to degrade transverse strength. When a plate is loaded transversely under uniaxial compression a single full-length imperfection would have the same form as the buckle pattern. Furthermore, the initial amplitude of the pressure-induced deflection would be enlarged by the application of the transverse membrane load. These two actions would tend to drive the plate combined stress (membrane plus bending) to the yield strength thereby producing premature buckling.

The premature loss of buckling strength in the heart of the transversely compressed long plate should have little effect upon the ultimate strength, however, since the post-buckling stress in that zone would be small.

Biaxial Strength

When a plate is subjected to biaxial membrane loading the effect of normal pressure would depend upon the relative proportions of the longitudinal and transverse loads. This can be seen in Figures 17 through 21. It would appear that a go-no-go situation exists. There seems to be a critical pressure below which the biaxial plate strength is not affected by normal pressure and above which the strength is driven to a lower value which appears to lie in the region of the elastic interaction curve for biaxially loaded plates. The mechanism of this process is not clear. Calculations have shown that the transitional condition occurs when transverse membrane and the bending stresses reach σ_{cy}. However, as was pointed out above, the stresses exist in the heart of the plate where, under uniaxial transverse compression, there is little post-buckling transverse stress in a long plate. On the other hand, the longitudinal loading could induce a sinusoidal buckle pattern which may inhibit the collapse of the plate under the transverse loads through the initiation of a series of node lines that act in the manner of transverse stiffeners. If the normal pressure is strong enough to drive the nodes to a stress intensity equal to yield then the plate should collapse. Otherwise, the biaxial strength will be achieved in spite of the normal pressure. This is an obvious area for further study.

MATERIAL COMPARISONS

Introduction

It is the purpose of this discussion to indicate the influence of compressive yield strength on the ultimate uniaxial compression strengths of plates fabricated from different materials. It must be emphasized that these comments and conclusions pertain only to compression and not to tension.

The fundamental information utilized in this discussion is the stress-strain curve. Once the basic mechanisms for plate strength are identified, the detailed evaluation of a given configuration requires the knowledge of the stress-strain curve.

Optimum Material for Thick Plates

Two steels with widely different yield strengths were used in this investigation for obtaining experimental data. The stress-strain curves appear in Figure II-2. Consider a plate thickness such that the critical strain is large enough to enter the yield regions for both materials. This would be true for simply supported rectangular plates with b/t = 30, for example. The longitudinal critical strain would be 4,000 μ. For perfect plates compressive load-carrying capacity is essentially the compressive yield strength. However, it is more realistic to assume that ship plates will not be perfect. If the total degradation strain is subtracted from the perfect-plate critical strain the result would be a relatively small strength loss for the weaker steel. However, depending upon the magnitude of the subtractive strains, a large strength loss can occur in the stronger steel. This result was observed in the current experiments.

One implication is that in a real ship structure the proportionate gain in compressive load-carrying capacity, when considering the use of a high-strength steel, may be considerably less than the increase in yield strength over that of a weaker steel. The yield strength increase for the two steels of Figure II-2 was 150%.The increase in plate strength was less than 60%. Essentially the same increase could have been obtained using a material with a yield strength of approximately 70 ksi and a sharp knee (n = 20 or more).

Another implication is that the evaluation of relative structural performances can be made with no more information than the compression stress-strain curve for each material under consideration. This assumes that the phenomenology of plate strength and the associated degrading factors are now understood well enough to permit these material comparisons.

The preceding discussions are related to the strength of the plates alone. Ship plating is stiffened. The load-carrying capacity of the combination could depend more on the stiffening system than on the plate. If the strength of the grillage depends primarily on the strength of the stiffening system as a set of columns then the above comments again would apply. The plastic strength of a column is closely related to the

tangent modulus of the column material. Consequently, the critical strain under that condition would force the effective strength to the left on each of the stress-strain curves. For most high-strength steels the knee is rounded somewhat in the manner shown for 4130 steel. Once again, the gain in load-carrying capacity may be significantly less than the gain in yield strength.

Identification of Optimum Material

The preceding discussions have provided the background for the selection of an optimum material for compression strength of plate. As in the previous cases this pertains to uniaxial compression alone.

Suppose it is desired to determine the properties of a steel that would operate more effectively to resist compression. The first step would be the selection of plate proportions for very high loadings which would correspond to b/t of the order of 30. The next steps would be to draw the Young's modulus line on graph paper (Figure 23) and to mark off the critical strain on the strain axis. For many materials the critical strain can be approximated by $\varepsilon_{cr} = (t/b)^2$ so that $\varepsilon_{cr} = 0.0033$. If a vertical line is drawn at that strain value it will intersect the Young's modulus line at the stress level for a perfect plate.

Now reduce the strain level by the total degradation strain values. On the basis of the data from this investigation that might be of the order of 0.001. The net strain is then 0.0023. If a vertical line is drawn at that strain it will intersect Young's modulus at a stress level of approximately 70 ksi, assuming E = 30 msi.

This would be the largest practical yield strength for a steel with a sharply rounded knee on the basis of the foregoing discussions.

When buckling occurs in the plastic range, the parameter F may be used to assess the change in ultimate strength with σ_{cy}. Since σ_{xu}/σ_{cy} decreases with increased σ_{cy} more or less in the manner shown in Figure 7 then it is clear that increased σ_{cy} implies decreased σ_{xu}/σ_{cy} for a given b/t and E for 1/F in the range between 2 and 6, say. At smaller F the value of σ_{xu}/σ_{cy} would be independent of σ_{cy}. However, this range would involve b/t values which may be impractical for ship construction.

Some of the information in the literature indicates attainment of a higher fraction of yield strength for the stronger steels than was observed in the current studies on 4130 steel. These are traceable to the plate restraints during testing.

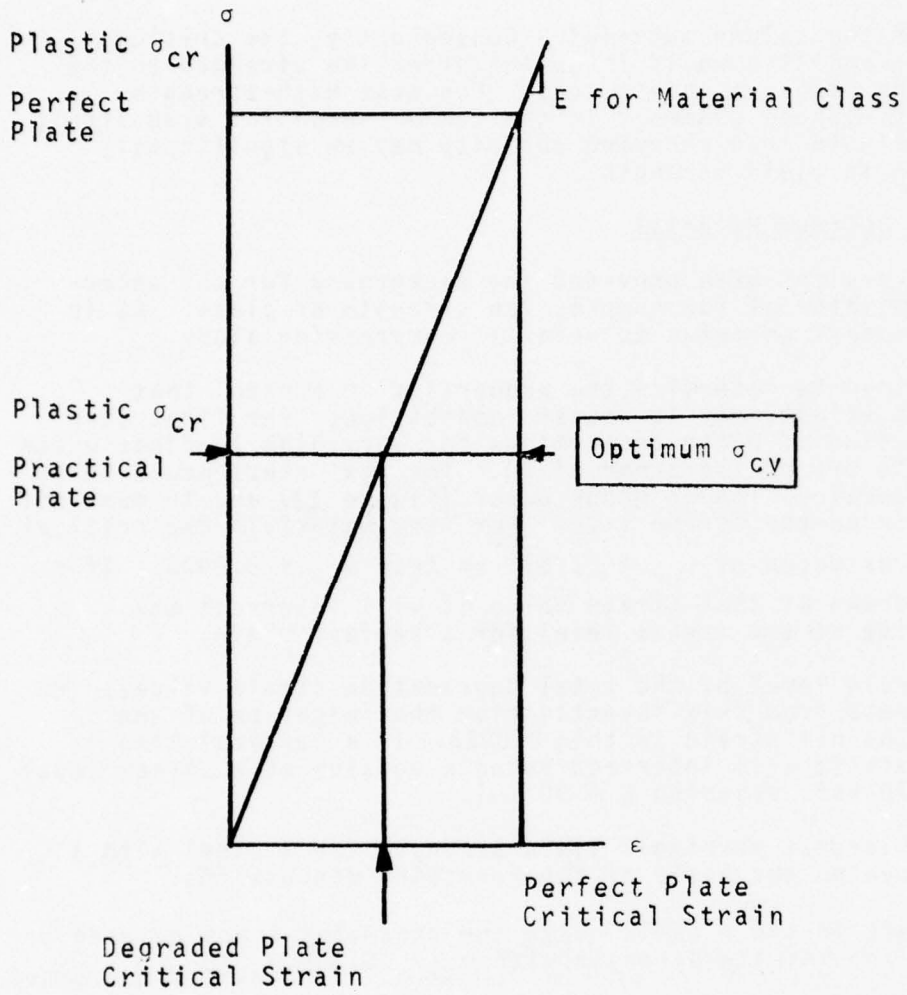

FIGURE 23 DETERMINATION OF OPTIMUM YIELD STRENGTH FOR PRACTICAL PLATES FABRICATED FROM GIVEN CLASS OF MATERIALS

GRILLAGE FAILURE MODES

Introduction

The major portion of this research has been on rectangular flat plates. This section discusses the manner in which that information fits into the overall problem of ship hull girder strength. The various modes of instability failure are examined and the relation of plate strength to hull strength is indicated.

Panel Failure

When a grillage is composed of longitudinally stiffened plates supported by transverses, the strength of the panel between the transverses may be controlled by the column action of the plate-stiffener system. That is to say, if the plate strength exceeds the strength of the stiffeners acting as columns (together with whatever effective plate width is brought into play) then panel failure may be the instability mode provided that all other failure modes have greater attainable stress levels. The column failure is assumed to occur in the same manner as a block cross-section column. Twisting and crippling would not be a source of concern for this type of failure. In a column the change from the straight state to the bent state is sudden. Furthermore, there is no mechanism that would permit the column to carry any significant load beyond the critical value. Therefore, column failure under a dead load is synonymous with buckling.

Stiffener Torsional Failure

Another possible instability mode would involve the rotation of the stiffeners between transverses. This could occur if the stiffeners presented a slender cross section with a narrow flange. The resultant movement of the flange translation perpendicular to the stiffener web and parallel to the plane of the plate as well as rotation about a longitudinal axis would result in another mode of collapse of the stiffening system and therefore of the panel between transverses.

Crippling

The stiffeners may have sufficient column strength and sufficient torsional rigidity to stabilize the plating and withstand panel failure to a high enough level for design purposes. However, it is important to insure a still higher level for stiffener flange buckling, which is a form of a general type of failure known as crippling. This type of instability almost invariably would take place in the plastic range. As a result flange buckling would be equivalent to flange failure.

General Instability

If the transverses are relatively light frames then the possibility exists that the entire grillage will be subjected to instability in the manner of an orthotropic plate. This type of buckling probably would be synonymous with failure. Theoretically, the application of proper boundary conditions to the grillage edges could permit the grillage to carry load beyond general instability in a manner similar

to that in which a plate can have a strength greater than the buckling stress. However, in the proportions of a practical ship, such a situation is unlikely.

Role of Plate

If the stiffeners are small then it would be reasonable to expect that plate strength would equal panel strength, or perhaps general instability strength. If the stiffeners are large with column strengths considerably greater than the plate ultimate strength then the role of the plate may be small in controlling the panel strength and also general instability. There would need to be an effort to identify the properties of the transition between those two extremes. For example, it is necessary to know whether plate buckling would tend to degrade the column strength of the stiffener to any extent. At present, this influence may be considered small. It is probably considerably less than for a stiffened cylinder for which the effect first was identified.

Loadings

In the preceding discussions of this section the loading has implicity been assumed to be longitudinal compression only. Detailed examinations have not been made of grillages loaded in biaxial compression. Only a small amount of work has been done on any phase of biaxial compression loading on plates. Therefore, it is not possible to identify reliably the interaction of the plate with the stiffening system for such a load field. If shearing stresses were to be imposed in addition to biaxial loading, the problem is more complicated. The presence of the tension field in a shear buckling situation exerts a radical influence upon the movements of the grillage boundaries and brings into play a strong interaction with the side shell that does not occur for longitudinal compression.

Comparison of Failure Modes

In terms of overall bending strength of the ship hull girder, it is clear that a number of failure modes must be investigated to determine the manner in which the grillage would be expected to exhibit instability. The edges of a plate are usually considered to reach material yield strength at the time the plate fails. Consequently, all failure modes of the stiffening system must achieve at least that same stress level and still be stable in order to drive the plate to the maximum load carrying capability.

It now remains to find a simple method of comparing the individual strengths as identifed above. This is achieved most effectively through the critical strain approach employing the stress-strain curve. It also is possible to utilize materials for stiffeners which have greater strength than materials used for plates. In this manner, it may be possible to operate the stiffeners in the elastic range while the plate boundaries are at stresses in the neighborhood of the yield strength of the plate material.

The mode comparisons would be made by identifying the critical strain for each type of instability identified above. The criterion for the relative strain magnitudes would be stipulated by the structural designer. This process would be the most effective way to identify effectively the order of failure of grillage components made of mild steel, which has a flat tangent modulus in the yield region.

CONCLUSIONS

The major conclusions to be drawn from the results of this investigation are as follows:

1. The basic theory of biaxial strength agrees well enough with experiments to be useful for ship design. However, the experimental foundation should be amplified with careful attention paid to controlling the boundary conditions and to identifying those which act on plates in a ship.

2. In general, one set of strength curves is required for each structural material covering the practical range of residual stresses and initial imperfections from perfect plates to poor plates.

3. The compression stress-strain curve is indispensable in evaluating plate strength, and conclusions about strength prediction could be in error if only the parameter, $1/F = (b/t)(\sigma_{cy}/E)^{1/2}$, is used.

   In that connection, the critical strain approach provides a simple means of accounting for strength degrading phenomena, which appear to be confined to reduction of the critical strength component of the ultimate strength.

4. It is possible to identify the yield strength of an optimum steel (or other material) for ship construction using stress-strain curves.

5. Plastic buckling in the yield range is synonymous with collapse. For a material with a relatively sharp knee the loss of strength from degrading factors would be small compared to the strength loss for elastically buckling plates.

6. The effects of normal pressure are predictable for uniaxial compression. The mechanism for biaxial compression needs further study.

RECOMMENDATIONS

1. The biaxial strength groundwork should be tested in ship-section structural models of larger scale than those employed during these investigations. In each test sufficient instrumentation should be provided to establish plate boundary conditions.

2. Compression stress-strain curves should be determined for the range of ship structural materials in use and contemplated. Enough samples of each material should be tested to identify the size of the scatter band for statistical analysis.

3. Attempts should be made to incorporate realistic stress-strain curve properties in fundamental mathematical strength analyses such as the application of finite-element computerization to plastic variational theory.

4. Experiments on the influence of normal pressure on biaxial strength should be designed and conducted to amplify the data base.

5. Design studies should be promulgated to determine procedures for optimizing structures for biaxial strength. Both minimum weight and minimum cost criteria should be used. Also, existing ships should be investigated to determine whether they have adequate biaxial strength for the intended missions.

APPENDIX I - EXPERIMENTS AND DATA

Specimen Characteristics

In this series of experiments almost all specimens were 0.025-inch thick 4130 steel plates electron-beam welded into square cross-section box tubes with a/b = 3, 1.5 and 1.0. Width/thickness, b/t, was 30 and 70. Two tubes were made from 1/16-inch thick 1010 carbon-steel plates with b/t = 70. The test specimen dimensions for the current series are shown in Figure I-1. Details of the 1010 steel specimens of the previous investigation appear in Reference 1.

The compressive stress-strain curves are shown in Figure II-2. The test procedure was the same as in the previous study (Reference 1) except for a modification to the transverse loading fixture described below.

The current transverse strength tests and biaxial compression tests were conducted on 4130 steel specimens with end plates. Figure I-2 depicts the range of end fixtures studied and shows the dimensions of the plates selected for the test program.

Load-Application Devices

The test equipment was essentially the same as in Reference 1. Minor modifications were required for the stainless steel specimens which were 0.025 inches thick compared to the 0.030 inch thick mild steel specimens tested in Reference 1. In addition, the transverse loading fixture was redesigned with the purpose of achieving more uniform loading on all four sides.

The new transverse load device was a compressive whiffletree which spread a single concentrated load into forces at eight equally spaced pads for a/b = 3 and into four pads for a/b = 1.5. The details are shown in Figures I-3 and I-4.

The whiffletree arrangement was employed to achieve maximum uniformity of transverse loading along the length of the specimen. It was anticipated that this also would result in more uniform distribution of forces into each of the four plates in the square tube.

Data Acquisition

Membrane forces and tube internal pressures were measured through gages described in Reference 1 and were recorded manually. The same is true of strain during the trepanning studies to measure residual stresses. The strain data and the load for stress-strain curve determination were recorded autographically.

Experimental Errors (Current Series)

The extreme variation in thickness was 2 percent but the mass of data yielded a variation of less than 1 percent. The largest departure from the nominal width (b/t = 30 was 2 percent. All others were of the

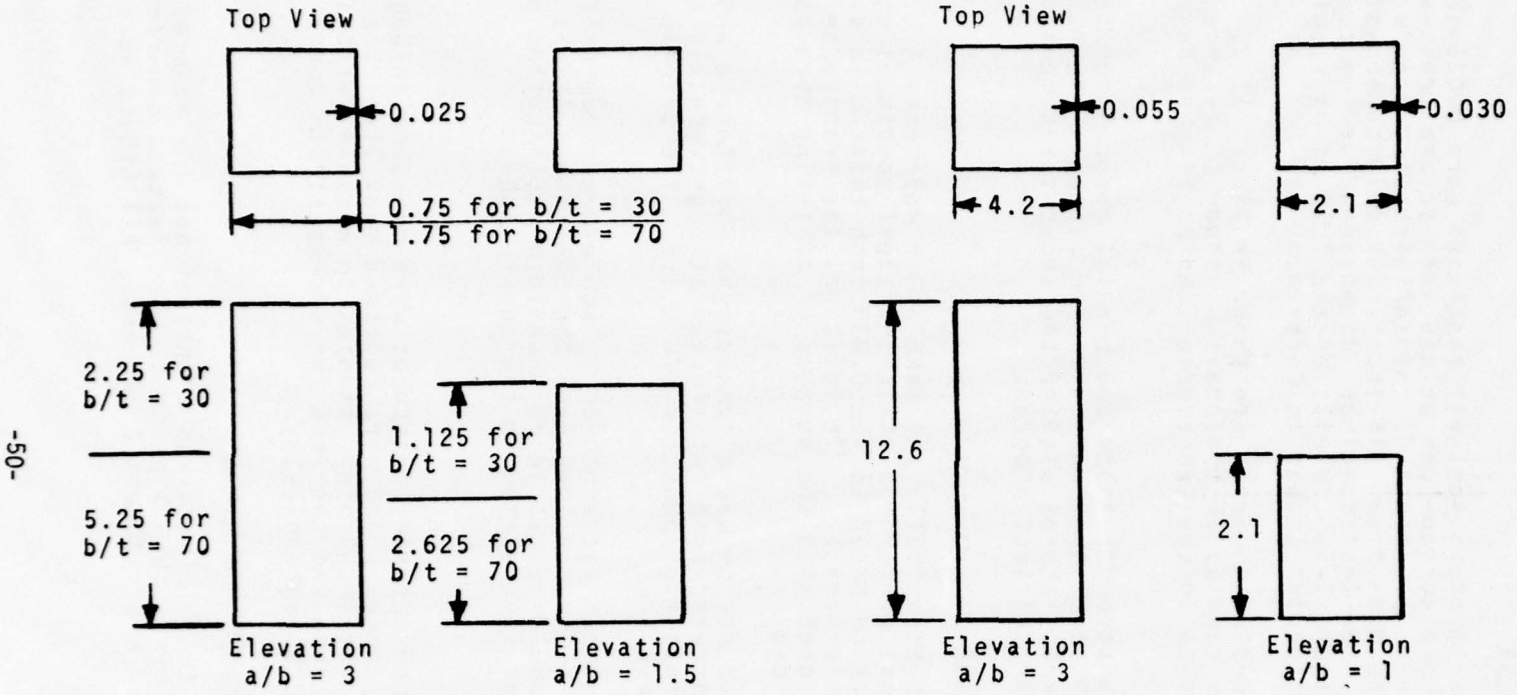

FIGURE I-1 SPECIMENS NOMINAL DIMENSIONS, CURRENT INVESTIGATION

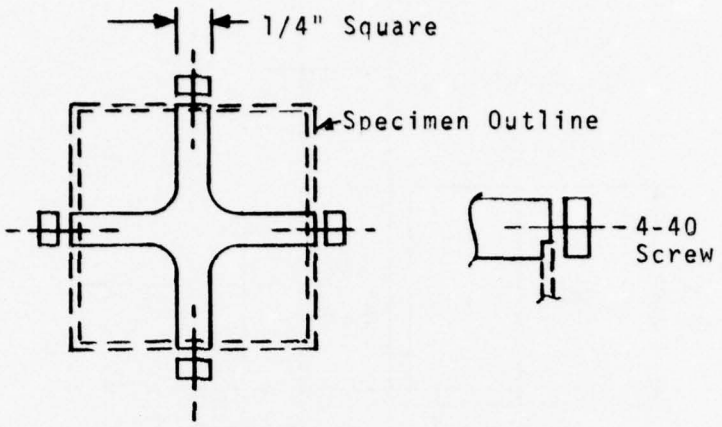

a. Cruciform (Schematic)

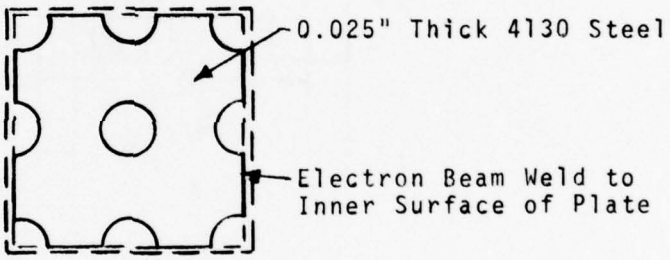

b. Locally Attached Plate (Schematic)

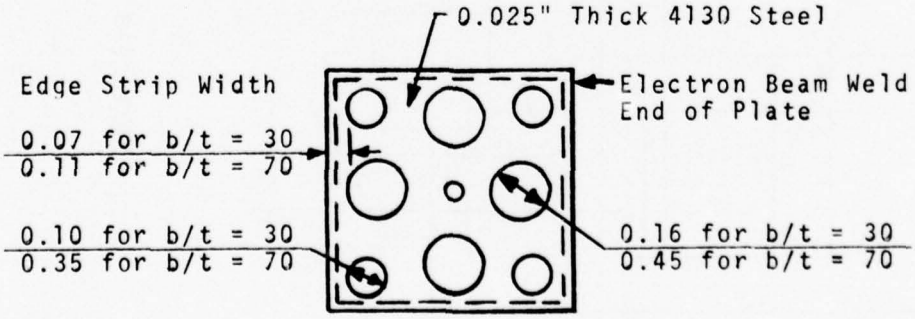

c. Final Design Perforated Cover Plate

FIGURE I-2 END PLATE CONFIGURATIONS

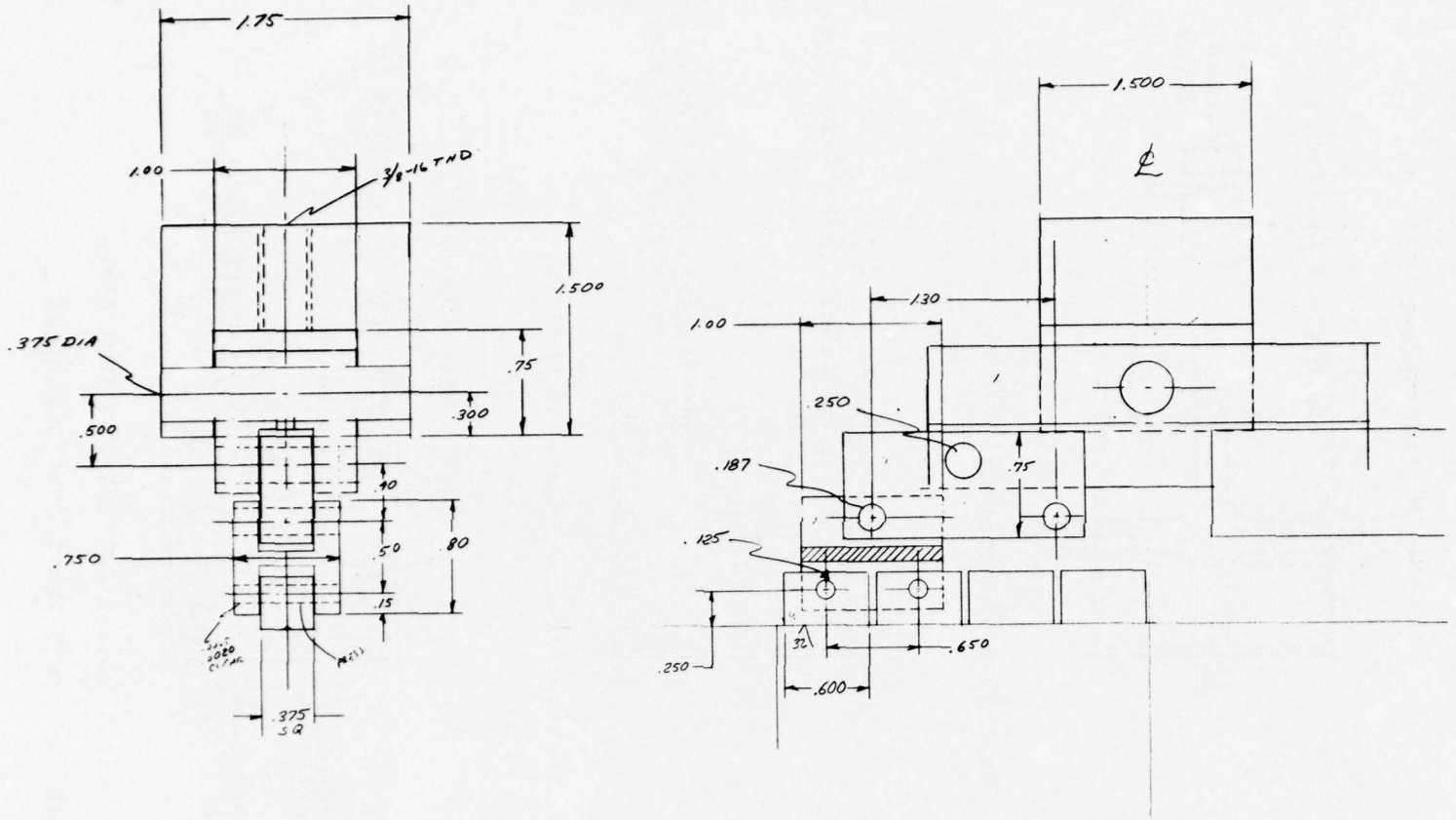

FIGURE I-3 · WHIFFLETREE FOR TRANSVERSE LOADING OF 4130 SPECIMENS WITH b/t = 70

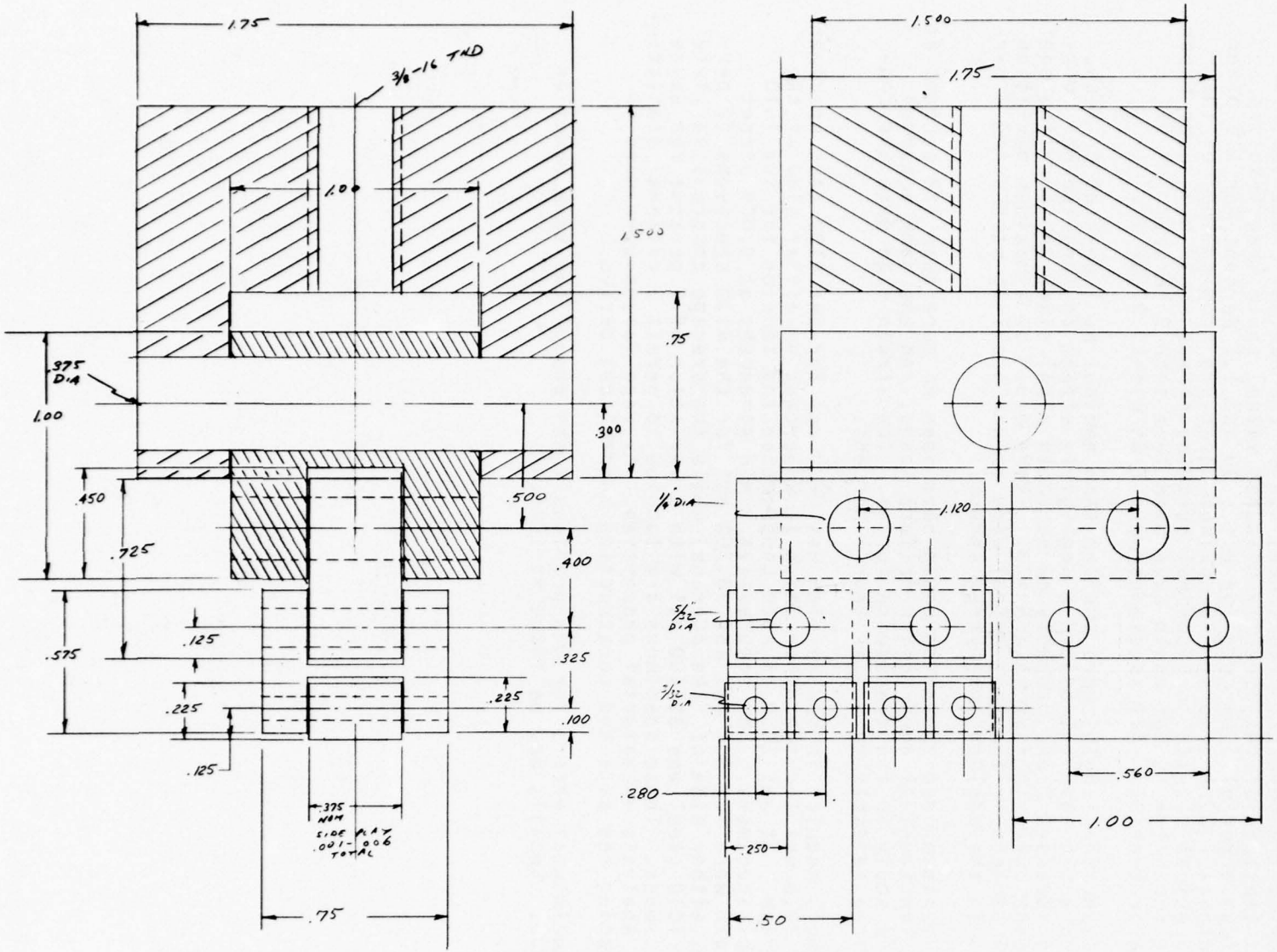

FIGURE I-4 WHIFFLETREE FOR TRANSVERSE LOADING OF 4130 SPECIMENS WITH b/T = 30

order of 1/2 percent. Therefore, use of the nominal cross-section area (instead of the directly measured value) could have involved a maximum error of 3 percent for b/t = 30 and 1.5 percent for all other specimens. Furthermore, the maximum departure from nominal of the theoretical elastic longitudinal buckling stress could have been 6 percent for b/t = 30 but would have been less than 3 percent for b/t greater than 30. All specimens were flat within 0.002 in.

All specimen lengths were smaller than nominal by 1 percent or less, which would have introduced a negligible effect on longitudinal buckling stresses (and probably on strength also) since the buckling coefficient curve is flat at a/b = 3. There could be a maximum deviation of 4 percent in the theoretical wide column buckling stress and 2 percent in the applied transverse stress.

The maximum load variation could have been no more than 1/2 percent at the longitudinal compression failure loads, and the same accuracy would apply to the transverse forces. The strain gage data are considered reliable to better than 1 percent.

Young's modulus in compression was 28.8 msi for one 4130 test specimen and 30.0 msi for the other which is 2 percent on either side of the average. It was 29.0 in both compression and tension for the 1010 steel specimens. The compressive yield strengths at 0.002 offset strain were 102,500 psi and 98,700 psi for the 4130 specimens (2 percent either side of the average) while the average compressive yield for 1010 steel was 39,400 psi with a variation of 2 percent for seven specimens. These specimens are too few to permit a rational statistical analysis on material properties. Average values were used in reducing the data and constructing theoretical curves.

Experimental errors for the previous tests are of the same order as above. Details may be found in Ref. 1.

TABLE I-1 STRENGTH DATA FOR 1010 STEEL SPECIMENS OF REFERENCE 1: a/b = 3, t = 0.030 in.

ALL WELDED

b/t	Model No.	P_x lb.	P_y lb.	p[a] psi	Load Sequence	σ_x[b] ksi	σ_y[c] ksi
30	1-30-7	4060	-	-	N_x	36.91	-
30	1-30-8	3810	-	10.6	pN_x	36.63	-
30	1-30-11	2420	2600	-	N_xN_y	23.30	22.80
30	1-30-12	800	3400	-	N_xN_y	7.70	29.80
30	1-30-14	1350	3600	-	N_xN_y	13.00	31.50
30	1-30-17	2800	3200	-	N_xN_y	26.90	28.00
30	1-30-16	-	3040	-	N_y	-	26.60
30	1-30-2	4000	1335	-	c	38.50	11.70
50	1-50-6	5500	-	-	N_x	30.47	-
50	1-50-7	5330	-	10.6	pN_x	30.46	-
50	9-50-15	5540	1510	-	N_yN_x	31.60	7.94
50	9-50-12	-	2100	-	N_y	-	11.02
50	9-50-11	4800	2000	-	N_yN_x	27.40	10.50
50	9-50-13	2960	2600	-	N_xN_y	16.88	13.65
50	9-50-17	3500	1800	-	N_yN_x	19.95	9.46
50	1-50-16	2960	3500	10.4	N_xpN_y	16.90	18.40
50	1-50-18	-	2660	9.9	pN_y	-	14.00
50	9-50-14	1380	2680	-	N_xN_y	7.88	14.10
50	1-50-19	3580	2240	30	N_xpN_y	20.40	11.77
70	2-70-3	5060	-	-	N_x	20.32	-
70	7-70-5	5260	-	10.6	pN_x	21.30	-
70	7-70-1	5060	-	-	N_x	20.32	-
70	8-70-13	3800	2940	-	N_xN_y	15.39	11.04
70	8-70-15	2530	2610	-	N_xN_y	10.24	9.81
70	10-70-18	1270	2990	-	N_xN_y	5.14	11.22
70	2-70-6	-	1470	-	N_y	-	5.53
70	2-70-16	3800	2440	10.9	N_xpN_y	15.39	9.18
70	7-70-12	2530	2440	10.3	N_xpN_y	10.24	9.18
70	2-70-19	1270	2480	10.5	N_xpN_y	5.14	9.32
70	10-70-17	-	1500	10.0	pN_y	-	5.64
70	7-70-14	2530	2300	16.	N_xpN_y	10.24	8.64
90	9-90-1	5250	-	-	N_x	16.43	-
90	10-90-3	5360	-	-	N_x	16.65	-
90	8-90-5	5090	-	10.6	pN_x	16.00	-
90	9-90-4	5130	-	10.5	pN_x	16.11	-
90	3-90-8	2650	3860	-	N_xN_y	8.34	11.28
90	3-90-11	2650	2290	11.6	N_xpN_y	8.34	6.69
90	10-90-7	3980	3690	-	N_xN_y	12.50	10.78
90	3-90-18	3980	2000	10.8	N_xpN_y	12.50	5.85
90	8-90-10	1330	3480	-	N_xN_y	4.18	10.16
90	8-90-9	1330	2535	10.6	N_xpN_y	4.18	7.40
90	8-90-6	-	1520	10.5	pN_y	-	4.44
90	3-90-19	-	1325	-	N_y	-	3.87
90	8-90-12	2650 530	2230 3200	-	e	8.34 1.67	6.53 9.34
90	6-90-16	2650	2340	10.6	N_xN_{yp}[f]	8.34	6.84

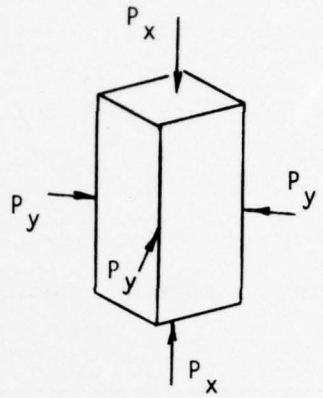

a Internal vacuum except for 1-50-19 (30 psi internal pressure), and 7-70-14 (16 psi internal pressure)

b $P_x/[4bt(1 - t/b)]$

c $0.707\ P_y/3bt$

d σ_x + 15.0 ksi, σ_y + 11.7 ksi, σ_x + 38.5 ksi (Failure)

e σ_x + 8.341 ksi, σ_y + 6.531 ksi, σ_x + 1.67 ksi, σ_y + Failure

f Failed 1 to 2 minutes after vacuum was applied

g All internal pressure

h Welded and Normalized

j Welded

TABLE I-1 CONTINUED STRENGTH DATA FOR 4130 STEEL SPECIMENS, a/b = 3, t = 0.025 in.

b/t	Model No.	P_x lb.	P_y lb.	p[g] psi	Load Sequence	σ_x[b] ksi	σ_y[c] ksi
30	1-1[h]	4070	-	-	N_x	57.08	-
30	1-2[h]	3900	-	-	N_x	54.55	-
30	1-3[h]	-	2810	-	p	-	37.28
30	1-31[h]	1000	3150	30	$N_x pN_y$	14.12	40.94
30	1-4[h]	3000	2520	15	$N_x pN_y$	42.08	35.58
30	1-5[h]	3000	2430	15	$N_x pN_y$	41.61	31.82
30	5-1[j]	4000	-	-	N_x	54.12	-
30	5-2[j]	4220	-	30	pN_x	58.12	-
30	5-3[j]	-	2500	-	N_y	-	31.79
30	5-31[j]	2000	3510	-	$N_x N_y$	-	46.74
30	5-4[j]	400	2925	-	$N_x N_y$	-	36.35
30	5-5[j]	-	2295	-	N_y	-	29.45
30	5-51[j]	3600	3555	-	$N_x N_y$	-	46.90
70	2-1[h]	5050	-	-	N_x	30.06	-
70	2-2[h]	4200	2205	-	$N_x N_y$	25.20	12.57
70	2-3[h]	-	2000	-	N_y	-	11.13
70	2-31[h]	3750	2205	10	$N_x pN_y$	22.42	12.37
70	2-4[h]	1250	2250	20	$N_x pN_y$	7.43	12.95
70	2-5[h]	-	1695	-	N_y	-	9.51
70	2-51[h]	6170	1080	-	$N_y N_x$	37.73	6.01
70	4-1[j]	4540	-	-	N_x	26.58	-
70	4-2[j]	5030	-	30	pN_x	30.05	-
70	4-3[j]	-	2020	-	N_y	-	11.38
70	4-31[j]	500	2250	-	$N_x N_y$	3.01	12.95
70	4-4[j]	2500	2475	-	$N_x N_y$	14.82	13.89
70	4-5[j]	4240	1683	-	$N_x N_y$	25.12	9.33

TABLE I-2 SHORT PLATE DATA

WELDED 4130 STEEL, a/b = 1.5, p = 0

b/t	P_x lb.	P_y lb.	σ_x ksi	σ_y ksi	t in.
30	5950	-	86.74	-	0.025
30	-	2420	-	63.61	0.025
70	7840	-	46.36	-	0.025
70	-	3330	-	35.89	0.025

WELDED 1010 STEEL, a/b = 1.0, p = 0

b/t	P_x lb.	σ_x ksi	t in.
30	3830	36.62	0.030
30	3790	36.03	0.030
70	6480	25.92	0.030
70	6885	27.65	0.030

TABLE I-3 THICK PLATE DATA

b/t	P_x lb.	σ_x ksi	t in.
80	22,200	24.46	0.055
80	19,500	21.45	0.055

APPENDIX II-THE STRESS-STRAIN CURVE

Plastic buckling theory utilizes several geometric properties of the stress-strain curve which are delineated in Figure II-1a. Ramberg and Osgood (Ref. 23) showed that, for typical structural metals, the curve is identifiable mathematically by 3 parameters; the tangent at the origin (which is usually termed Young's modulus, E), the stress level, σ_1, at which the secant modulus is 0.70E, and the sharpness of the knee, n, defined in Figure II-1b. Table II-1 displays these parameters for various materials of interest to ship construction.

Material	σ_{cy} ksi	E msi	σ_1 (range) ksi	n (range)	E/σ_{cy}	$(E/\sigma_{cy})^{1/2}$
Mild Steel to HY-80	32	29	29.7 31.1	20 50	906	30.1
	39	29	35.7 37.4	15 30	744	27.3
	60	29	55.7 57.5	12 20	483	22.0
	80	29	73.1 75.8	10 16	363	19.0
Alum. Alloy	40	10	39.1 39.4	8 12	250	15.8

TABLE II-1 REPRESENTATIVE COMPRESSIVE MECHANICAL PROPERTIES OF SELECTED STRUCTURAL MATERIALS

The stress-strain curves for the steels of SSC-217 and the current studies appear in Figure II-2. Each is an average from autographic recordings of two measurements. The three parameters are shown for each material.

The 3-parameter description shows that

$$E/E_s = 1 + (3/7)(\sigma/\sigma_1)^{n-1} = 1 + (3/7)(\sigma/\sigma_{cy})^{n-1}(\sigma_{cy}/\sigma_1)^{n-1} \quad \text{(II-1)}$$

$$E/E_t = 1 + (3n/7)(\sigma/\sigma_1)^{n-1} = 1 + (3n/7)(\sigma/\sigma_{cy})^{n-1}(\sigma_{cy}/\sigma_1)^{n-1} \quad \text{(II-2)}$$

from which it is a simple matter to derive the result

$$E_t/E_s = \frac{1 + (3/7)(\sigma/\sigma_1)^{n-1}}{1 + (3n/7)(\sigma/\sigma_1)^{n-1}} \quad \text{(II-3)}$$

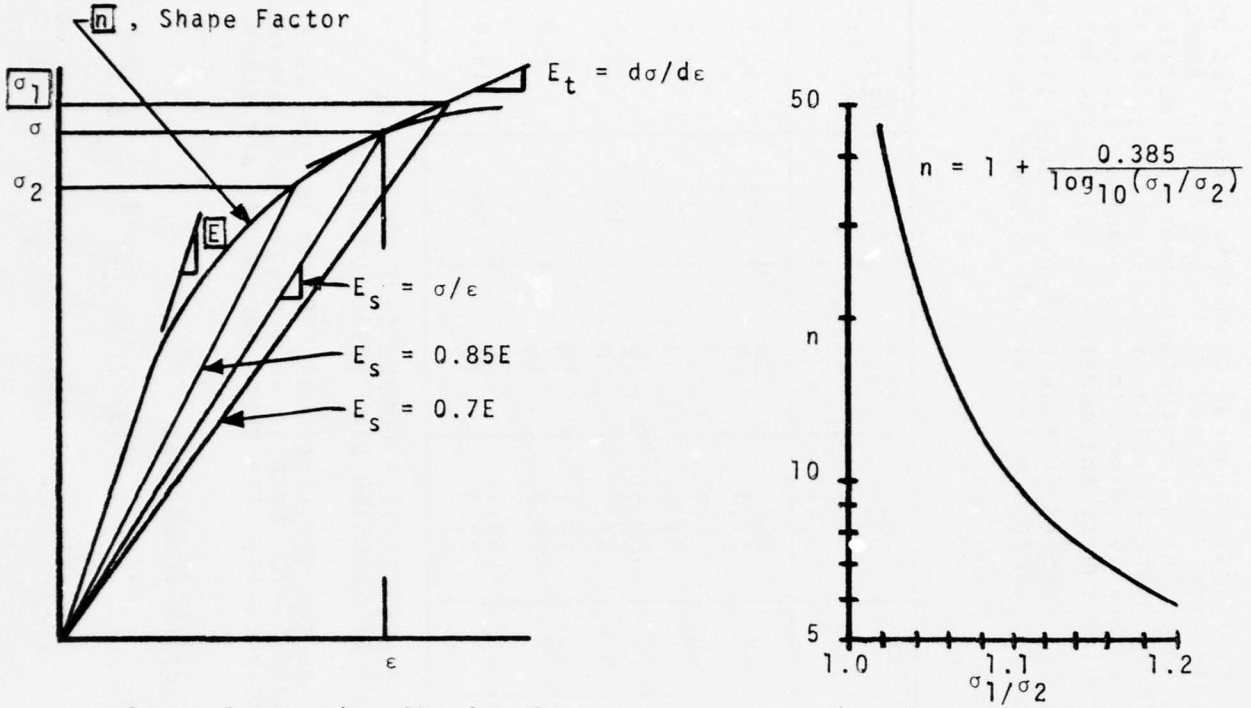

a. Curve Properties Showing 3 Parameters of Ramberg and Osgood

b. Determination of n

FIGURE II-1 THREE PARAMETER DESCRIPTIONS OF STRESS-STRAIN CURVES

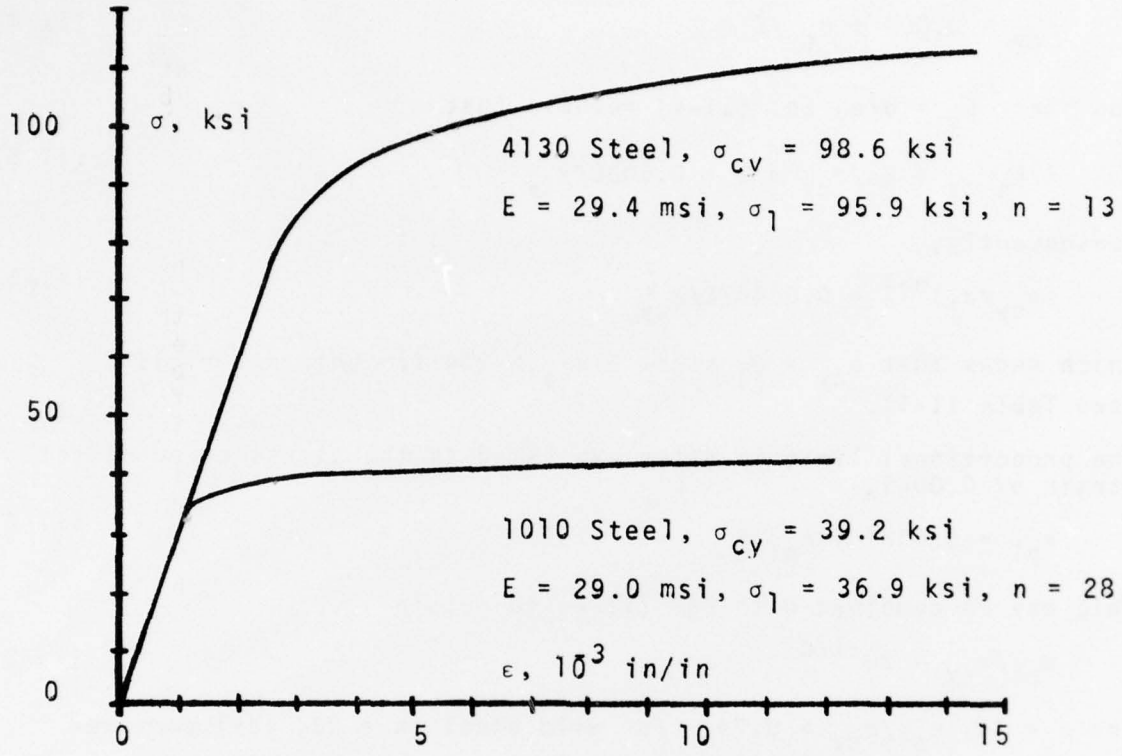

FIGURE II-2 STRESS-STRAIN CURVES FOR MATERIALS USED IN REFERENCE 1 AND THE CURRENT INVESTIGATIONS

From the conventional definition of the compressive yield strength, σ_{cy}, the compressive yield strain is

$$\varepsilon_{cy} = 0.002 + \sigma_{cy}/E \tag{II-4}$$

and since $E_s = \sigma/\varepsilon$, Eq. (II-4) reveals that

$$E/E_{s\ cy} = E\varepsilon/\sigma_{cy} = 1 + 0.002E/\sigma_{cy} \tag{II-5}$$

Consequently,

$$(\sigma_{cy}/\sigma_1)^{n-1} = 0.00467E/\sigma_{cy} \tag{II-6}$$

which shows that $\sigma_{cy} > \sigma_1$ since $E/\sigma_{cy} > 214$ for ship materials (see Table II-1).

The proportional limit is often expressed as the stress at an offset strain of 0.0001,

$$\varepsilon_{pl} = 0.0001 + \sigma_{pl}/E \tag{II-7}$$

This may be combined with Eq. (II-4) to obtain

$$\sigma_{pl}/\sigma_{cy} = 20^{-1/n} \tag{II-8}$$

For $n = 10$, $\sigma_{pl}/\sigma_{cy} = 0.74$. For mild steel ($n = 20$, say) compared to high strength steel ($n = 10$, say)

$$(\sigma_{pl}/\sigma_{cy})_{n=20}/(\sigma_{pl}/\sigma_{cy})_{n=10} = 1.162$$

This result becomes significant when materials are compared for compressive efficiency.

APPENDIX III POLYAXIAL PLASTIC BUCKLING

General Solutions

An approach to the analysis of plastic buckling in flat plates was presented by Stowell (Ref. 20). The analyses in this section make use of his differential equation for rectangular plates

$$C_1\partial^4 w/\partial x^4 - C_2\partial^4 w/\partial x^3\partial y + 2C_3\partial^4 w/\partial x^2\partial y^2 - C_4\partial^4 w/\partial x\partial y^3 + C_5\partial^4 w/\partial y^4 + (N_x/D')\partial^2 w/\partial x^2 + 2(N_{xy}/D')\partial^2 w/\partial x\partial y + (N_y/D')\partial^2 w/\partial y^2 = 0 \qquad \text{(III-1)}$$

using $D' = E_s t^3/9$ and in which w is the out-of-plane movement.

A tractable solution for a simply supported plate in biaxial compression (and also shear under certain conditions) has been employed in the form (with x in the a-direction and y in the b-direction).

$$w = w_o \sin[(m\pi/a)(x + \zeta y)]\sin(\pi y/b) \qquad \text{(III-2)}$$

which assumes one-half wave in the y direction. When substituted into Eq. (III-1),

$$C_1(m\pi/a)^4 - C_2\zeta(m\pi/a)^4 + 2C_3(m\pi/a)^2[(\zeta m\pi/a)^2 + (\pi/b)^2] - C_4\zeta(m\pi/a)^2[(\zeta m\pi/a)^2 + 3(\pi/b)^2] + C_5\{[(\zeta m\pi/a)^2 + (\pi/b)^2]^2 + 4\zeta^2 m^2\pi^4/a^2b^2\} = (N_x/D')(m\pi/a)^2 + 2(N_{xy}/D')(m\pi/a)^2 + (N_y/D')[(\zeta m\pi/a)^2 + (\pi/b)^2] \qquad \text{(III-3)}$$

The coefficients are as follows

	In the plastic region	In the elastic region
C_1	$1 - \frac{3}{4}(\sigma_x/\sigma_i)^2(1 - E_t/E_s)$	$C_1 = 1$
C_2	$3(\sigma_x\tau/\sigma_i^2)(1 - E_t/E_s)$	$C_2 = 0$
C_3	$1 - \frac{3}{4}[(\sigma_x\sigma_y + 2\tau^2)/\sigma_i^2](1 - E_t/E_s)$	$C_3 = 1$
C_4	$3(\sigma_y\tau/\sigma_i^2)(1 - E_t/E_s)$	$C_4 = 0$
C_5	$1 - \frac{3}{4}(\sigma_y/\sigma_i)^2(1 - E_t/E_s)$	$C_5 = 1$

using (with $r = \sigma_y/\sigma_x$)

$$\sigma^2_i = \sigma_x^2 + \sigma_y^2 - \sigma_x\sigma_y + 3\tau^2 = \sigma_x^2(1 - r + r^2) + 3\tau^2$$

When shearing stresses are absent, $\zeta = 0$ and Eq. (III-3) reduces to the biaxial compression case.

Stowell tabulated plasticity reduction factors for a variety of loadings. These have been reproduced in Table III-1. Results appear below for shear, biaxial compression and transverse compression.

STRUCTURE	j
Long flange, one unloaded edge simply supported	1
Long flange, one unloaded edge clamped	$0.330 + 0.335(1 + 3E_t/E_s)^{1/2}$
Long plates, both unloaded edges simply supported	$0.50 + 0.25(1 + 3E_t/E_s)^{1/2}$
Long plate, both unloaded edges clamped	$0.352 + 0.324(1 + 3E_t/E_s)^{1/2}$
Short plate loaded as a column ($a/b \ll 1$)	$0.25 + 0.75E_t/E_s$
Square plate loaded as a column ($a/b = 1$)	$0.114 + 0.886E_t/E_s$
Long column ($a/b \gg 1$)	E_t/E_s

TABLE III-1 PLASTICITY REDUCTION FACTORS AFTER STOWELL

Shear Buckling

In the elastic case, Eq. (III-3) becomes

$$N_{xy}b^2/\pi^2D' = k_{xy} = (1/\zeta)\{(1/2)u(1 + \zeta^2)^2 + 1 + 3\zeta^2 + 1/2u\} \quad \text{(III-4)}$$

This is exactly the same relation, presented by Timoshenko (Ref. 11), which was based on the use of energy procedures. Through minimization, $\zeta = (2)^{-1/2}$ and $u = 2/3$. These yield $k_{xy} = 5.66$, which is 6 percent greater than the infinite series value of 5.35.

Eq. (III-4) applies to infinitely long plates. For plates of finite length, the expression

$$k_{xy} = 9.34 - 4.00(1 - b/a)^{1/2} \qquad \text{(III-5)}$$

gives a somewhat better fit than that presented by Timoshenko.

For plastic shear buckling,

$$k_{xy} = (1/\zeta)[(u/2)(1 + 2C_3\zeta^2 + \zeta^4) + 3\zeta^2 + (1/2u) + C_3] \qquad \text{(III-6)}$$

The minimization process involves matching α and u to C_3. Since this result is not of immediate consequence to the current project, no further action will be taken here on shear plastic buckling.

Biaxial Compression Buckling

With $\zeta = 0$ and utilizing $N_y = rN_x$,

$$(b^2N_x/\pi^2D')[(mb/a)^2 + r] = C_1(mb/a)^4 + 2C_3(mb/a)^2 + C_5 \qquad \text{(III-7)}$$

where $C_1 = 1 - (3/4)(1 - r + r^2)^{-1}(1 - E_t/E_s)$

$C_3 = 1 - (3/4)r(1 - r + r^2)^{-1}(1 - E_t/E_s)$

$C_5 = 1 - (3/4)r^2(1 - r + r^2)^{-1}(1 - E_t/E_s)$

When $N_y = 0$, Eq. (III-7) reduces to the frequently used result for uniaxial plastic compressive buckling (Table III-1).

In the elastic range, Eq. (III-7) is the biaxial relation presented by Timoshenko (Ref. 11).

$$(b^2N_x/\pi^2D')[(mb/a)^2 + r] = [(mb/a)^2 + 1]^2$$

When $r = N_y = 0$,

$$k_x = b^2N_x/\pi^2D = (a/mb + mb/a)^2$$

When $N_x = N_{xy} = 0$,

$$C_1 = C_3 = 1,\ C_2 = C_4 = 0, \text{ and } C_5 = 1/4 + (3/4)(E_t/E_s) \qquad \text{(III-8)}$$

For a wide plate m = 1 and

$$N_y b^2/\pi^2 D' = 1/4 + 3/4(E_t/E_s) + (b/a)^4 + 2(b/a)^2 \qquad \text{(III-9)}$$

In the elastic range Eq. (III-9) reduces to the relation for a plate of finite a/b > 1. For large a/b the last two terms are discarded and the wide-column plasticity reduction factor of Table III-1 is obtained.

In the above results the term D' is used. For slightly greater precision D can be used if the general expression for σ_{cr} is written.

$$\sigma_{cr} = k(\pi^2 D/b^2 t)[(1 - \nu_e^2)(1 - \nu^2)](E_s/E)j \qquad \text{(III-10)}$$

in which the appropriate value of j is obtained from Table III-1.

The plasticity reduction factor then would be

$$\eta = [(1 - \nu_e^2)/(\sigma - \nu^2)](E_s/E)j \qquad \text{(III-11)}$$

where

$$\nu = 0.5 - 0.2\, E_s/E \qquad \text{(Ref. 25)} \qquad \text{(III-12)}$$

REFERENCES

1. Becker, H., R. Goldman, J. Pozerycki and A. Colao, "Compressive Strength of Ship Hull Girders, Part I - Unstiffened Plates". U. S. Ship Structure Committee Report SSC-217, 1970. AD 717590.

2. Becker, H., "Feasibility Study of Model Tests on Ship Hull Girders". U. S. Ship Structure Committee Report SSC-194, May 1969. AD 687220.

3. von Karman, T., E. Sechler and L. Donnell, "The Strength of Thin Plates in Compression". Journal of Applied Mechanics, v. 54, 1932, p. 53ff.

4. Bengtson, H. W., "Ship Plating Under Compression and Hydrostatic Pressure". Trans. SNAME, v. 47, no. 80, 1939, pp. 80-116.

5. Duffy, D. J. and R. B. Allnutt, "Buckling and Ultimate Strengths of Plating Loaded in Edge Compression. Prog. Rep. No. 1, 6061-T6 Aluminum Plates". DTMB Report 1419, April 1960.

6. Gerard, G., "Secant Modulus Method for Determining Plate Instability Above the Proportional Limit". Journal of Aeronautical Sciences, v. 13, no. 1, January 1946, pp. 38-44, 48.

7. Dwight, J. B. and A. T. Ractliffe, "The Strength of Thin Plates in Compression", Published in "Thin-Walled Steel Structures", Ed. by Rockey and Hill, Gordon and Breach, N. Y., 1969, pp. 3-34.

8. Moxham, K. E., "Buckling Tests on Individual Welded Steel Plates in Compression". Cambridge University Report CUED/C-Struct/TR.3, 1971.

9. Dwight, J. B. and A. P. Dorman, "Tests on Stiffened Compression Panels and Plate Panels". STEEL BOX GIRDERS - Proceedings of the London International Conference, 13-14 February 1973, Session B, Paper 5, pp. 63-75, Institution of Civil Engineering, London.

10. Jubb, J. E. M., I. G. Phillips and A. Panas. Several Reports in Process of Publication.

11. Timoshenko, S., "Theory of Elastic Stability". McGraw-Hill, 1936.

12. Vasta, J., Unpublished U. S. Experimental Model Basin Progress Reports , ca 1940.

13. Moxham, K. E., "Theoretical Prediction of the Strength of Welded Steel Plates in Compression". Cambridge University Report CUED/C-Struct/TR.2, 1971.

14. Dawson, R. G. and A. C. Walker, "A Proposed Method for the Design of Thin-Walled Beams which Buckle Locally". The Structural Engineer, v. 50, no. 2, February 1972, pp. 95-105.

15. Coan, J. M., "Large-Deflection Theory for Plates with Small Initial Curvature Loaded in Edge Compression". Journal of Applied Mechanics, v. 18, no. 2, June 1951, pp. 143-151.

16. Faulkner, D., "Compression Strength and Chance". Component of M.I.T. Report on Ship Structural Design Concepts, Cornell Maritime Press, Inc., Cambridge, MD. 1975.

17. Mansour, A. E. and D. Faulkner, "On Applying the Statistical Approach to Extreme Sea Loads and Ship Hull Strength". Trans. Royal Institute of Naval Architects, v. 115, 1973, pp. 277-314.

18. Stowell, E. Z., "Compressive Strength of Flanges". NACA TN 2020, 1950.

19. Gerard, G., "Handbook of Structural Stability. Part IV - Failure of Plates and Composite Elements". NACA TN 3784, August 1957.

20. Stowell, E. Z., "A Unified Theory of Plastic Buckling of Columns and Plates". NACA TR 898, 1947.

21. McPherson, A. E., S. Levy and G. Zibritosky, "Effects of Normal Pressure or Strength of Axially Loaded Sheet-Stringer Panels". NACA TN 1041, July 1946.

22. Gerard, G. and H. Becker, "Handbook of Structural Stability. Part III - Buckling of Curved Plates and Shells". NACA TN 3783, August 1957.

23. Ramberg, W. and W. R. Osgood, "Description of Stress-Strain Curves by Three Parameters". NACA TN 902, July 1943.

24. Ractliffe, A. T., "The Strength of Plates in Compression". Cantab Ph.D. Thesis, October 1968.

25. Gerard, G. and Wildhorn,S."A Study of Poisson's Ratio in the Yield Region". NACA TN 2561, January 1952.

UNCLASSIFIED
Security Classification

DOCUMENT CONTROL DATA - R & D

Security classification of title, body of abstract and indexing annotation must be entered when the overall report is classified)

1. ORIGINATING ACTIVITY (Corporate author) Naval Ship Engineering Center	2a. REPORT SECURITY CLASSIFICATION UNCLASSIFIED 2b. GROUP

3. REPORT TITLE

COMPRESSIVE STRENGTH OF SHIP HULL GIRDERS - PART III - THEORY AND ADDITIONAL EXPERIMENTS

4. DESCRIPTIVE NOTES (Type of report and inclusive dates)

Final Report

5. AUTHOR(S) (First name, middle initial, last name)

H. Becker and A. Colao

6. REPORT DATE	7a. TOTAL NO. OF PAGES	7b. NO. OF REFS
April 1977	66	25

8a. CONTRACT OR GRANT NO. N00024-72-C-5565 new	9a. ORIGINATOR'S REPORT NUMBER(S)
b. PROJECT NO. SR-206	
c.	9b. OTHER REPORT NO(S) (Any other numbers that may be assigned this report) SSC-267 ✓
d.	

10. DISTRIBUTION STATEMENT

This document has been approved for public release and sale; its distribution is unlimited.

11. SUPPLEMENTARY NOTES	12. SPONSORING MILITARY ACTIVITY Naval Sea Systems Command

13. ABSTRACT

A phenomenological theory has been developed for predicting the ultimate strength of rectangular structural plates loaded in uniaxial longitudinal compression, uniaxial transverse compression and biaxial compression. The effects of normal pressure also were considered.

The theory was found to be in reasonable agreement with experimental data. Certain areas of the theory and some of the experiments require additional study.

The longitudinal compression theory was found to agree well with corresponding theories of other investigators. However, the new theory employs the detailed stress-strain curve for a given material, which the others do not, and demonstrates that, in general, strength prediction requires a curve for each structural material. The commonly used parameter, $(b/t)(\sigma_{cy}/E)^{1/2}$, is shown not to be universally employable across the total material spectrum as the factor identifying ultimate strength.

Other results of broad interest are the demonstration of the applicability of a biaxial plasticity law to biaxial strength theory and the delineation of a method for selecting an optimum material for compression strength.

The use of stress-strain curves for strain analysis of critical and ultimate strengths is described. They were employed to construct theoretical strength curves.

Theoretical relations and corresponding curves have been developed for perfect plates. The effects of strength degrading factors are discussed and the analysis of residual stress effects is included.

DD FORM 1 NOV 65 1473 (PAGE 1)

S/N 0101-807-6801

UNCLASSIFIED
Security Classification

* U.S. GOVERNMENT PRINTING OFFICE : 1977 O-730-678/660

SHIP RESEARCH COMMITTEE
Maritime Transportation Research Board
National Academy of Sciences-National Research Council

The Ship Research Committee has technical cognizance of the interagency Ship Structure Committee's research program:

PROF. J. E. GOLDBERG, Chairman, *School of Civil Engrg., Georgia Inst. of Tech.*
DR. J. M. BARSOM, *Section Supervisor, U.S. Steel Corporation*
MR. D. P. COURTSAL, *Vice President, DRAVO Corporation*
MR. E. S. DILLON, *Consultant, Silver Spring, Maryland*
DEAN D. C. DRUCKER, *College of Engineering, University of Illinois*
PROF. L. LANDWEBER, *Inst. of Hydraulic Research, The University of Iowa*
MR. O. H. OAKLEY, *Consultant, McLean, Virginia*
MR. D. P. ROSEMAN, *Chief Naval Architect, Hydronautics, Inc.*
DEAN R. D. STOUT, *Graduate School, Lehigh University*
MR. R. W. RUMKE, *Executive Secretary, Ship Research Committee*

The Ship Design, Response, and Load Criteria Advisory Group prepared the project prospectus and evaluated the proposals for this project:

MR. D. P. ROSEMAN, Chairman, *Chief Naval Architect, Hydronautics, Inc.*
PROF. A. H.-S. ANG, *Dept. of Civil Engineering, University of Illinois*
PROF. S. H. CRANDALL, *Dept. of Mech. Engrg., Massachusetts Inst. of Technology*
DR. D. D. KANA, *Manager, Struct. Dynamics & Acoustics, S.W. Research Institute*
MR. W. J. LANE, *Structural Engineer, Bethlehem Steel Corporation*
DR. M. K. OCHI, *Research Scientist, Naval Ship Research & Development Center*
PROF. W. D. PILKEY, *Dept. of Mechanics, University of Virginia*
PROF. H. E. SHEETS, *C'man, Dept. of Ocean Engineering, Univ. of Rhode Island*
MR. H. S. TOWNSEND, *Consultant, Westport, Connecticut*
PROF. G. A. WEMPNER, *School of Engrg. Science & Mechanics, Georgia Inst. of Technology*

The SR-206 Project Advisory Committee provided the liaison technical guidance, and reviewed the project reports with the investigator:

PROF. J. E. GOLDBERG, Chairman, *School of Civil Engrg., Georgia Inst. of Tech.*
MR. J. VASTA, *Senior Consultant, Litton Systems, Inc.*
PROF. G. A. WEMPNER, *School of Engrg. Science & Mechanics, Georgia Inst. of Technology.*

SHIP STRUCTURE COMMITTEE PUBLICATIONS

These documents are distributed by the National Technical Information Service, Springfield, Va. 22151. These documents have been announced in the Clearinghouse journal U.S. Government Research & Development Reports (USGRDR) under the indicated AD numbers.

SSC-253, *A Guide for the Nondestructive Testing of Non-Butt Welds in Commercial Ships - Part One* by R. A. Youshaw and E. L. Criscuolo. 1976. AO-14547.

SSC-254, *A Guide for the Nondestructive Testing of Non-Butt Welds in Commercial Ships - Part Two* by R. A. Youshaw and E. L. Criscuolo. 1976. AD-A014548.

SSC-255, *Further Analysis of Slamming Data from the S.S. WOLVERINE STATE* by J. W. Wheaton. 1976. AD-A021338.

SSC-256, *Dynamic Crack Propagation and Arrest in Structural Steels* by G. T. Hahn, R. G. Hoagland, and A. R. Rosenfield. 1976. AD-A021339.

SSC-257, (SL-7-5) - *SL-7 Instrumentation Program Background and Research Plan* by W. J. Siekierka, R. A. Johnson, and CDR C. S. Loosmore, USCG. 1976. AD-A021337.

SSC-258, *A Study to Obtain Verification of Liquid Natural Gas (LNG) Tank Loading Criteria* by R. L. Bass, J. C. Hokanson, and P. A. Cox. 1976. AD-A025716.

SSC-259, (SL-7-6) - *Verification of the Rigid Vinyl Modeling Technique: The SL-7 Structure* by J. L. Rodd. 1976. AD-A025717.

SSC-260, *A Survey of Fastening Techniques for Shipbuilding* by N. Yutani and T. L. Reynolds. 1976. AD-A031501.

SSC-261, *Preventing Delayed Cracks in Ship Welds - Part I* by H. W. Mishler. 1976. AD-A031515.

SSC-262, *Preventing Delayed Cracks in Ship Welds - Part II* by H. W. Mishler. 1976. AD-A031526.

SSC-263, (SL-7-7) - *Static Structural Calibration of Ship Response Instrumentation System Aboard the Sea-Land McLean* by R. R. Boentgen and J. W. Wheaton. 1976. AD-A031527.

SSC-264, (SL-7-8) - *First Season Results from Ship Response Instrumentation Aboard the SL-7 Class Containership S.S. Sea-Land McLean in North Atlantic Service* by R. R. Boentgen, R. A. Fain and J. W. Wheaton. 1976. AD-A039752.

SSC-265, *A Study of Ship Hull Crack Arrester Systems* by M. Kanninen, E. Mills, G. Hahn, C. Marschall, D. Broek, A. Coyle, K. Masubushi and K. Itoga. 1976. AD-A040942.

SSC-266, *Review of Ship Structural Details* by R. Glasfeld, D. Jordan, M. Kerr, Jr., and D. Zoller. 1977. AD-A040941.